Lawrence Berkeley National Laboratory
Recent Work

Title
STRUCTURE AND HIGH STRENGTH METALS

Permalink
https://escholarship.org/uc/item/7g8128t7

Authors
Thomas, G.
Zackay, V.F.
Parker, E.R.

Publication Date
1965-08-01

University of California

Ernest O. Lawrence
Radiation Laboratory

STRUCTURE AND HIGH STRENGTH METALS

Berkeley, California

DISCLAIMER

UCRL-16301

UNIVERSITY OF CALIFORNIA

Lawrence Radiation Laboratory
Berkeley, California

AEC Contract W-7405-eng-48

STRUCTURE AND HIGH STRENGTH METALS

G. Thomas, V. F. Zackay, and E. R. Parker

August 1965

STRUCTURE AND HIGH STRENGTH METALS

G. Thomas, V. F. Zackay, and E. R. Parker[†]

INTRODUCTION

While the profession of engineering is almost as old as civilization, the age of materials science spans only a few decades. Engineers have long been accustomed to building safe and reliable structures by the empirical knowledge accumulated from experience. Even now structural materials operating in extreme and complex environments are selected more by empiricism than be predictions based upon fundamentals. This is especially true when complex mechanical properties such as fatigue, notch toughness, and stress-corrosion are involved. However, the gap between empiricism and under-standing is now being closed at an ever increasing rate.

A cursory glance at the progress made during the past three decades reveals that now there is almost a complete atomistic understanding of the underlying mechanisms of plastic flow in simple solids. Furthermore, pro-gress has also been rapid in important allied fields such as alloy theory and phase transformations.

The)application of this knowledge to the design of superior materials has already begun (see e.g. refs 1,2).

It is the purpose of this paper to summarize briefly what is known about the plastic behavior of simple solids in terms of atomistic processes. The emphasis is on the relatively uncomplicated but important properties of strength and ductility. The limitations of the principal strengthening mechanisms are delineated and optimum procedures for achieving very high

[†]Inorganic Materials Research Division, Lawrence Radiation Laboratory and Department of Mineral Technology, College of Engineering, University of California, Berkeley, California.

strength in complex solids are suggested. Some of the progress made to date in achieving these goals is reviewed. Since the literature concerned with structure and strength is so voluminous, typical bibliographical references are cited where appropriate.

SOME FUNDAMENTAL CONSIDERATIONS OF HIGH STRENGTH

Metallic crystals are plastic because either they contain dislocations that can move or because dislocations are created easily under applied stresses.[3,4] This is why metals such as copper and aluminum are "soft" and deform plastically at very low stress levels (10^{-4} to 10^{-5} G).[*] The geometrical requirement for plasticity is that crystals contain at least five independent slip systems in order to mitigate the stress concentrations of groups of blocked dislocations. This criterion is easily met by cubic crystals, but not necessarily for hexagonal metals where the critical resolved shear stress is so high for some modes that they remain inactive. An ideally perfect crystal would be purely elastic up to stress levels that would either break the crystal or cause dislocations to be generated spontaneously. The theoretically shear strength of close packed crystals has been estimate to be about one-fifteenth of the shear modulus.[3] Thus, the corresponding stress in a tensile test would be equal to twice the value of the theoretical shear strength. The only materials with strengths approaching theoretical values are whiskers, which are exceptionally small specimens of pure materials made so that they are highly perfect. Some measured pro-

---

[*] In this paper G always refers to the shear modulus.

perties of small crystals are shown in Table I. In ordinary large pieces of materials many defects are present within the crystals and the materials are correspondingly weak.

Because it is not possible to prepare large pieces of metals without grain boundaries or other defects at which dislocations can be generated (and made to move and multiply under the application of small stresses) other means are adopted to strengthen materials. This is done by utilizing obstacles, such as other dislocations, grain boundaries, or particles of second phases in the paths of moving dislocations. The kinds of barriers needed to impede the movement of dislocations most effectively are well known but it is often difficult to produce microstructures containing ideal barriers. Furthermore, engineering materials must be made with sufficient ductility to provide safety in operation and thus requires that some visibility of dislocations be allowed. Thus, there must be a compromise between strength and ductility. If dislocation motion is too strongly impeded, the material may be too brittle for use in an engineering application. A certain minimum amount of plastic flow is essential to relieve the high local stresses present around stress concentrations, such as notches, in order to ensure safe performance.[5]

A reasonable approximation for the yield strength in terms of barriers is given in simplest form by the following, well known, Orowan equation:[6]

$$T_y \cong Gb/L \text{ (shear)} \qquad \qquad 1 \text{ (a)}$$

$$\cong 2Gb/L \text{ (shear)} \qquad \qquad 1 \text{ (b)}$$

where L is the longest mean free path of a mobile dislocation of Burger's vector, b. That is, L is the separation between dislocations or other

barriers in the slip plane. For tensile loading, the theoretical limit of strength is equal to the shear modulus divided by 7.5. Thus the limit of L is about fifteen Burger's vectors, or about 75Å units for aluminum. If the corresponding limit of strength could be achieved, the metal would necessarily be brittle. From the above equation, it can be seen that the higher the shear modulus the greater is the potential for high strength.

Figure 1 is a plot of the tensile yield strength against the parameter $\frac{L}{b}$ to the upper limit of 0.15G. It is evident from this plot that the high modulus materials such as tungsten, molybdenum beryllium have the best potential for developing high yield strengths. The shear modulus is not the only factor of importance, however, because materials such as tungsten have high densities and are, consequently, not as effective per unit volume as the lighter elements, such as beryllium. The importance of the density factor is illustrated in Table II, where the ratio of the shear modulus to the density is shown in the fourth column. When the density is taken into account, tungsten, iron, molybdenum and aluminum all appear to be about equal. Beryllium, because of its low density and high modulus, appears to have about five times as high a potential as the previously mentioned metals. As is shown by the last column in Table II, there is still room for a great deal of improvement in the properties of commercial materials. The hope for improving strength resides in the possibility of controlling microstructure in such a way that, without significantly impairing ductility, the barriers to dislocations can be controlled in shape and nature, and shaped appropriately, to obtain higher strengths. A discussion of the factors that affect the mobility of dislocations in crystals is now in order.

One important property of dislocation that affects its mobility in crystals is its width. This refers to the distance in the crystal over which the change from the slipped to the unslipped state occurs. When this transition is wide, the dislocations can move with greater ease than when this zone is narrow. Narrow dislocations occur in strongly bonded crystals, such as those of diamond, silicon, and germanium. In such crystals, large stresses are required to make the dislocation move from one atomic position to another. The force required to move a dislocation against the bonding forces in a crystal is known as the frictional force, or the Peirls-Nabarro force. A simplified expression[4] for such a force is given in the following equation:

$$\tau = \frac{2G}{(1-\nu)} \varepsilon + \rho \left[-\frac{2\pi a}{b(1-\nu)} \right] \tag{2}$$

where a is the interplanar spacing, b is the Burger's vector and ν is Poisson's ratio. The stress required to move a dislocation increases rapidly as the ratio of $\frac{a}{b}$ increases, or, in other words, as the width of a dislocation decreases. In face centered cubic metals, which have low stacking fault energies, the dislocations are widely split into partials, as has been shown directly using electron microscopy by many investigators.[7] These partials have small Burger's vectors, and they are very mobile. Freidel[8] has pointed out an additional fact viz., in crystals where dislocations are dissociated into partials, and these partials are widely separated, the theoretical elastic limit should be lowered by a factor of about one-half. This is due to the lower activation energy required to nucleate a partial dislocation in contrast to that required for the generation of a whole dislocation, and this consideration is important when the stacking fault energy,

γ, is less than about 200 ergs/cm^2. On this basis, copper, silver, and gold are poor choices for base metals, but aluminum, nickel, and the body centered cubic metals are good choices. Furthermore, the velocities with which dislocations can move through crystals are related to their width. Experiments have shown that the velocity, v, of a dislocation is related to the applied stress, σ, by the following equation:[9,10]

$$\nu = [\sigma/\sigma_0]^n \qquad (3)$$

where n is in the range from 10 to 40 for body centered cubic metals, but is very large, of the order of 300, for face centered cubic metals. This effect, combined with the pinning of dislocations by impurities or precipitates accounts for the yield point phenomena.[9-11] Yield drops are expected when either the number of mobile dislocations suddenly increases (e.g. by multiplication) or when a higher stress is required to move a dislocation at a higher velocity. Such effects are well known in impure bcc metals and in non-metals[9] but yield points are rare in fcc metals. Thus, the stress strain curves for fcc and bcc crystals are often different, particularly during the initial stages of plastic flow. These are represented schematically in Fig. 2, while Fig. 3 shows results obtained on niobium of varying purity. Figure 3 indicates that the impurity effect overrides the grain size effect in controlling the yield strength. From a practical viewpoint, therefore, it may be very much more difficult to strengthen face centered or hexagonal close-packed metals than those with body centered cubic crystal structures, e.g., ferritic steels can be hardened to much higher strengths than austenitic alloys of low stacking fault energy.[12]

The onset of plastic flow requires that high enough stresses be applied to free dislocations from pinning obstacles. Continued plastic flow requires that stress levels sufficient such that dislocations can overcome barriers in their paths be applied. Important obstacles are listed below:[4,8]

1. The Peierls-Nabarro lattice friction stress which is important in covalently bonded crystals, in body centered cubic metals at very low temperatures, and in metals where dislocations do not lie in close-packed planes.

2. Dislocation forests, i.e. dislocations grown in or pre-existing in crystals through which moving dislocations must glide. (The interaction of moving dislocations with other dislocations that thread through the slip planes is thought to be one of the major causes of work hardening.[13,14]

3. The mutual elastic interaction of dislocations as they move near each other in their passage through crystals.

4. Grain boundaries, stacking faults, twin boundaries, or films on the external surfaces are all effective barriers to dislocation motion.

5. Solute atoms segregated to dislocation networks provide strong barriers to moving dislocations.

6. Foreign atoms, either clustered or existing in an ordered state, may offer considerable resistance to the motion of dislocations.

7. Among the most effective barriers are precipitated particles of second phases particularly intermetallic compounds (i.e. hard, refractory inclusions).

The strength of various obstacles depends upon the temperature of the deformation.[3,8,15,16] The shear modulus varies slowly with changing temperature and its effect can be evaluated by measuring the modulus vs temperature. The effects of thermally activated slip processes can be distinguished from the modulus effect because of their relatively larger temperature dependence. Obstacles generally create local stresses in the lattice, and if these local stresses do not extend over long distances thermal vibrations can assist dislocations in moving past the obstacles. If the internal stresses do extend over long distances, then thermal fluc- tuations are of no avail, and dislocations can only be forced to pass such obstacles by externally applied stresses. Examples of barriers with short range stress effects are the Peierls-Nabarro stress, forest or intersecting dislocation interactions, impurity atoms, short-range ordered regions, and small coherent precipitates. A strong temperature dependence of yield strength is always observed when such barriers influence the strength. Long range stress effects can arise from complex dislocation interactions, grain boundaries, large particles of a second phase and also possibly long-range ordering or clustering. The relative importance of barriers may change markedly with temperature, with some barriers being unimportant at high temperatures but assuming major importance at low temperatures.

Grain boundaries can act either as sources of strength or of weakness. Dislocations may be generated from grain boundaries during the early stages of yielding,[17] and thus contribute to weakness, but grain boundaries can also impede the motion of dislocations,[18] particularly if foreign atoms are present in the boundaries and thus contribute to strength.[17,18]

There is a marked grain size effect in many metals and alloys. This effect is indicated by the following equation:[19, 20]

$$\tau_y = \tau_i + k \, [d]^n \tag{4}$$

where σ_i is the friction stress which included all short-range obstacles, n is a factor ranging from about -1/2 to 1, and d is the average grain size. The parameter k varies widely from one metal to another and also depends upon the state of a particular metal. For grain size to be important in strengthening, d would have to be about 0.1 micron for high strength materials. However, the hardening effect predicted by Eq. 3 is not observed at very small grain sizes. Moreover, it is not practical and generally not possible to produce materials with very small grain sizes and, consequently, strengthening by decreasing the grain size is not generally a very effective way to raise the strength of metals.

Cold working is not only the oldest and simplest way of strengthening metals, but is also a very effective one; e.g. the yield strength can be raised over at least a six-fold range. Deformation strengthening is due to the complex interactions of dislocations with each other as the dislocations try to move through the lattice. Dislocations moving through a forest of other dislocations can undergo several types of interactions such as cutting, the production of jogs and point defects, the formation of junctions in networks, etc. The details of the interactions are complicated because of the large number of possible interactions that can occur (for review see ref. 14). Because of the stress fields that exist around dislocations, they can interact with each other, reducing the local stress fields and thus

produce a lower energy configuration which causes them to cease motion and become tangled. Tangled dislocations provide effective barriers to other moving dislocations. The result is the formation of complex networks of tangled dislocations which have been clearly revealed by transmission electron microscopy.[7] An example is shown in Fig. 4. The density of tangled dislocations increases with plastic deformation, and higher stresses must be applied to cause plastic flow to continue. The degree of tangling depends upon the amount of strain and upon the number of slip systems operating simultaneously. Figure 5, taken from the work of Mukherjee et al.,[21] shows that the rate of work hardening increases rapidly with the number of operating slip systems.

Most of the theories of work hardening predict a flow stress that is proportional to the square root of the total dislocation density.[3,8,13,14] This relationship has been found to hold by a number of investigators, for both face centered cubic and body centered cubic metals.[7] Saada[22] has suggested that the most likely athermal mechanism of hardening arises from gliding dislocations cutting forest dislocations at attractive junctions. In this case, the flow stress is given by:

$$\sigma_f = \frac{Gb}{BL_j} \tag{5}$$

where L_j is the mean distance between attractive junctions and B a geometrical factor of value about 2.5 for face centered cubic crystals. L_j is about twice the value of L which is the average spacing between all dislocations in the forest. Excellent agreement between Saada's model has been provided by the experiments of Mukherjee et al.[21] As L decreases with increasing dislocation density, the available sources of fresh dislocations becomes limited

to the network itself. Thus for high values of flow stress, the tangled networks can act either as barriers or sources.[17]

Electron microscope studies have shown that the maximum dislocation density produced by cold work is about $10^{12}/cm^2$. Such dislocations are concentrated in cell walls and are not uniformly distributed throughout the volume of the material. Crystals are divided into heavily dislocated boundaries surrounding relatively perfect cells (Fig. 4). It is reasonable to expect that with a structure such as this, the flow stress would depend upon the cell diameter, just as it does upon grain size. Warrington[23] has observed such an effect for copper, as is shown in Fig. 6. An extrapolation of his data indicates that to reach the theoretical limit of yield strength of 0.15 times the shear modulus, the cell size would have to be of the order of 0.1 micron. Such values have not yet been obtained in cold worked metals.

The effect of cell size on the hardness of nickel subjected to explosive deformation[24] is shown in Table III. The ratio of the hardnesses produced by the 250 kilobar and the 70 kilobar treatments is 1.52, which is close to the ratio of the corresponding square roots of the cell sizes, namely 1.73. The cell sizes produced by explosive deformation of nickel are smaller than those which could normally be produced by ordinary plastic deformation (which generally produces cell sizes no smaller than about half a micron). Such cells are shown in Fig. 7a-c and can be compared to the cells produced in nickel deformed by tensile straining in Fig. 4. A further complication is that cell walls of the type illustrated are not stable at elevated temperatures where dislocations can climb and move away from each other, and the cell walls

can untangle and disappear. In order to provide strength at high temperatures, the dislocations must be pinned by foreign atoms or particles. This process will be discussed in more detail in a later section. (The effect of grain size on cell size is probably due to the fact that boundaries act as sources and dislocations emanating therefrom interact after traveling shorter distances in the smaller grain material).

Heat Treatment Producing Work Hardening

Plastic deformation is not the only means of obtaining high dislocation densities. Shear, or martensite phase transformations occur with the formation of martensite which contains dislocations or twins due to the transformation strain.[7] The most widely known and investigated martensite transformation is that which occurs in iron based alloys. In these systems the transformation strain produces dislocations in martensites of relatively dilute alloys but with increasing solute content and the accompanying decrease in Ms temperature, which is the parameter that seems to control the transformation strain, there is an increase in amount of twinned martensite. While low carbon martensites do contain appreciable numbers of dislocations (similarly to heavily worked metals) the work hardening contribution can play a secondary role to carbon solution strengthening[7] but the combined effects of carbon and dislocations can lead to relatively high strengths (about 1/4 theoretical).[29] However, there is a limit to useful carbon levels since beyond about 0.3 to 0.4% C, the martensites become twinned and are embrittled. Furthermore, in plain carbon steels, tempering leads to rapid growth of cementite particles and loss of strength. Some benefit is realized by adding alloy carbide formers in which case the tempering results in precipitation of alloy carbides rather than cementite—such alloys are

then age-hardened.[12] The most striking development in high strength steels is the ausforming process which produces a highly work-hardened alloy which contains stable, finely dispersed precipitates of alloy carbides. These will be discussed in a later section. Cold working martensites also leads to strengthening, e.g. yield strengths of 400,000 psi in 0.4C steel have been reported.[35]

The application of ferrous martensite hardening has not been carried to non-ferrous alloys primarily because of the emphasis that has been given to the role of interstitial solutes in strengthening the bcc martensitic structure, and their small effects on hardening fcc and hcp structures. However, what has already been achieved for ferrous alloys might also be achieved in other bcc systems, if systems can be found which undergo martensitic transformations.

Some increase in hardness has been observed in Cu-Al martensites after aging. These martensites have complex faulted structures. Ordering is presumably responsible for the observed aging response. Such alloys have nearly double the strength of hard rolled copper, but, unfortunately, are also brittle.

Limitations of Work Hardening

From observations it is well known that the smallest cell size normally observed in cold worked materials is of the order of 1/2 micron.[4] The observed strengths of cold worked metals corresponds well with those predicted from the observed cell sizes. From Table II it can be seen that the observed maximum tensile strength of heavily deformed metals is about 0.4 of the theoretical, which corresponds to the value that is estimated from the observed cell sizes.

If work hardening were to be utilized to produce a maximum of strength, the critical value of L_j would be given by the following equation:

$$L_{j(critical)} \simeq \frac{Gb}{2.5\sigma_{theor.}} \simeq 7b \tag{6}$$

which corresponds to a dislocation density of about $10^{14}/cm^2$ in the cell walls (the limiting dislocation density in cubic crystals is $\sim 10^{15}/cm^2$). There is no practical way to obtain dislocation densities of this magnitude. However, it can be seen that if dislocation densities such as this could be produced, the strength of real metals could be raised to near the theoretical value. Thus, it may be concluded that high strength can be produced either in very perfect or highly imperfect crystals.

There is little hope that further improvements in strength can be obtained by normal cold working operations. The strain rate effect does, however, offer some promise. As illustrated in Figs. 4 and 7, explosive deformation produces smaller cell sizes than can be produced by normal static loading. However, it is now known that in face centered cubic metals no further reduction in cell size with further increase in explosive pressure is possible because at higher pressures twinning occurs instead of slip.[24] Mechanical twinning was observed in nickel subjected to pressures above 250 kilobars. Higher pressures produced no significant increase in hardness.[24] This, and other observations on martensites, strongly indicate that mechanical twinning does not contribute significantly to strengthening. In iron explosive deformation produces a phase transformation (see e.g. ref. 25).

Dispersion Strengthening

Dislocations multiply at different rates in different materials and in those materials in which the multiplication rate is greatest, the work

hardening rate is highest (see Fig. 3). Strain hardening can be fostered by the presence of barriers such as particles of intermetallic compounds. One phenomenon which contributes to dislocation multiplication is cross slip. Only dislocations with appreciable screw character can cross slip, and when they do, they move from one slip plane to an equivalent slip plane without changing the Burger's vector. Once a segment of a dislocation has cross slipped, it then will have part of its line lying in a different slip plane. The parts connecting the ends of this portion to the original dislocation in the original slip plane are unable to move or can move only with great difficulty, and consequently, the cross slipped length can act as a new Frank-Read source bowing out, sweeping through the crystal, and multiplying as originally postulated by Frank and Read. Dispersed particles acting as barriers to moving dislocations can force screw dislocations to cross slip and thus act as dislocation multiplication centers.

It is well known that dispersed particles increase the strength of a metal (for review see ref. 16). They do this in two ways: first by restricting the motion of dislocations on slip planes (causing them to bow out between the particles and requiring stresses proportional to $\frac{Gb}{L}$), and second, by causing dislocations to cross slip and multiply[16, 26-29] as sketched in Fig. 8. The dislocation tangles resulting therefrom causes the rate of work hardening to increase drastically as is commonly observed in precipitation hardening alloy systems.

The stress required to operate a source resulting from a cross-slip process is $\approx \frac{Gb}{d}$, where d is the particle diameter or the length of the cross-slipped portion of the dislocation. If d is very much less than L, this source cannot operate unless the stress is raised to a substantially

higher value than that required for bowing. It is only when the diameter
of the dispersed particle and the spaces between particles are the same
order of magnitude that both mechanisms can operate simultaneously. This
is presumably why the cells observed to form in alloy systems with dispersed
phases appear to have corners located at the largest particles. This is
illustrated for TD nickel in Fig. 9(a). The large effect of the substructure
on yield strength is shown in Fig. 9(b). When the particle diameter d
is less than the distance L between particles, during the initial stages of
plastic flow, dislocations will bow and move between particles or become heavily
jogged or cross-over rather than cross slip around them (i.e. the total length
of dislocation increases). As they do this they may leave behind loops and
debris, so that effectively the particles increase in size as deformation
proceeds. Eventually, then, the inter-particle spacing becomes reduced and
the effective particle diameter d_e increases until $d_e \approx L$, whence the material
begins to be most effectively work hardened. For the theoretical strength
plotted in Fig. 1 to be approached, the ratio of $\frac{L}{b}$ should be approximately
equal to $\frac{d}{b}$, and this in turn should be approximately equal to 15. However,
under these circumstances, substantially no plastic flow would occur and the
material would be brittle. From a practical point of view, the ideal dis-
persion necessary to produce high strength would be difficult to achieve and
their mechanical properties would not necessarily be optimum. If the particles
were of the order of 100 $\overset{\circ}{A}$ in diameter, they should produce strengths of about
half the theoretical while still leaving the material with something of
the order of 10% elongation.

The nature of the particles is also important. If the particles are
soft or coherent with the parent lattice, the dislocations may move through,

rather than around the particles and their effectiveness would thereby be diminished.[16] Even with particles of the intermetallic compound type, large differences may be observed, depending upon the mechanical properties of the particles.

The effects of different kinds of barriers on the stress-strain curve is illustrated in Fig. 10. If, in identical matrices, particles having a diameter, d, spaced a distance L apart existed, but in one the particles were ductile while in the other they were hard and strong, the two alloys would then exhibit the same yield strength (because this would be determined by the spacing between the particles), but the rate of work hardening would be drastically different in the two cases, as is shown by the comparison of curves 1 and 2 in the figure. Curve 3 indicates the behavior of the metal without the dispersed phase, the pure metal having a lower yield strength but the same rate of strain hardening as that of the material containing the soft dispersed phase.

It is of interest to note that although dispersed particles of a hard, strong phase are present, and that these increase the rate of strain hardening of the material due to augmented dislocation multiplication, they do not in real systems produce the necessary multiplication of dislocations required to reach the theoretical upper limit of strength. About 10^{14} dislocations per square centimeter would be necessary to produce the maximum strength in a cold worked material, but in real materials, even with dispersions present the maximum density is at least in order of magnitude lower than this value.

Strengthening in Fiber-Reinforced Composites

In the introductory section it was observed that, although pure metals

are usually weak, they have near-theoretical strength when in the form of "whiskers" or fibers. The possibility of strengthening metals at both low and elevated temperatures by the incorporation of high strength and high modulus fibers in metals has been the subject of active research in recent years. Current reviews of fiber-strengthening by Kelly and Tyson,[30] Davies,[31] and Kelly and Davies[32] summarize progress in this field. These papers serve as the primary source of information for this section and the reader is referred to them for a more detailed and comprehensive study.

One of the primary distinctions between dispersion and fiber strengthening is that of scale.[30] For effective dispersion strengthening the particles must serve as barriers to dislocation motion and the interparticle spacing must be of the order of microns, (i.e., always less than the grain size of the matrix). The mechanism of fiber strengthening is quite different. The composite is designed so that the applied load is transferred from the matrix to the fiber. The fibers do not significantly alter dislocation motion and their spacing is often greater than the grain size.

A few of the more important requisite properties of fibers can be mentioned. Fibers must have high tensile strengths and high modulus. The tensile strengths, moduli, strength-to-weight ratios, and melting points of representaitve whiskers, fibers, and wires, taken from the work of Kelly and Davies[32] are shown in Table I. For efficient transfer of stress from the matrix to the fiber, the fibers must be rods or plates with high aspect ratios, i.e., they must have high values of the ratio of length to thickness. The matrix must bind the fibers together yet keep them separate, it must protect the fiber surfaces from damage, and, for effective stress transfer it must deform plastically at stresses well below the working stress of the composite.

There are four distinct stages of deformation that are observed in the
stress-strain curve of a metal fiber-metal matrix composite.[32] There are:
(1) fibers and matrix deform elastically, (2) the fibers deform elastically
and the matrix deforms plastically, (3) the fibers and the matrix both deform
plastically, and (4) the fibers crack and the composite fractures. The
stress-strain curves of tunsten wire, bulk copper, and two tungsten wire-
copper composites (of varying volume fractions of fibers) are shown in Fig. 11.

Stage (2), which occupies most of the stress-strain curve, is the most
useful range. During this stage the modulus of the composite is given by

$$E_c = E_f V_f + \left(\frac{d\sigma_m}{d\varepsilon_m} \right)_\varepsilon \cdot V_m \tag{7}$$

where $\left(\frac{d\sigma_m}{d\varepsilon_m} \right)_\varepsilon$ is the slope of the stress-strain curve of the matrix at the

strain, ε, of the composite in stage (3). The quantity $\left(\frac{d\sigma_m}{d\varepsilon_m} \right)_\varepsilon$ is $\leq \frac{E_m}{100}$

for matrices of pure metals so far investigated; hence, for stage (2), the
modulus of the composite is given closely by $E_c = E_f V_f$, where V is the
volume, and the subscripts c, f, m refer to the composite, fiber, and matrix,
respectively.

The ultimate strength of a composite is reached at a strain equal to the
total strain of the fibers at their ultimate strength. The fibers are assumed
to be ductile and continuous. For these conditions the ultimate strength of
the composite is given by:

$$\sigma_c = \sigma_f V_f + \sigma_m' (1-V_f), \qquad V_f > V_{min} \tag{8}$$

where σ_f is the ultimate tensile strength of the fibers, σ_m' is the stress
of the matrix at the ultimate tensile strain of the fibers, and V_f and V_{min}
are the colume fraction and a critical volume fraction for strengthening of
the fibers, respectively.

If the fibers are _brittle_ and _continuous_, there is a critical volume fraction $V_{f\ crit}$ which must be exceeded for strengthening to occur. This can be shown to be:

$$V_{f\ crit} \geq \frac{\sigma_{w.h.}}{\sigma_f - \sigma_m}' \qquad (9)$$

where $\sigma_{w.h.}$ is the increase in flow stress caused by plastic working of the matrix. This value of $V_{f\ crit}$ is derived on the assumptions that for real systems the amount of work-hardening is large, that there is not interference by the fibers with dislocation motion, and, lastly, that when a fiber fails there is local work-hardening by the matrix to make up for the loss of load-bearing capacity. The maximum value for V_f for fibers of circular cross section is equal to 90 percent. Larger maximum values of V_f are possible for other shapes. For brittle fibers of circular cross section the strength falls off for volume fractions greater than 80 percent. This is probably due to the fibers coming into contact with each other. Values of the order of 80 percent seem to be the maximum practical value.

The above analyses have been based on the assumption that the fibers were continuous, but in a real composite the fibers are likely to be discontinuous. If the fiber length exceeds a critical length, l_c, then the strength of the composite is the same as that for one containing continuous fibers.

The critical length is defined as

$$l_c = d\sigma_f/2\tau \qquad (10)$$

where τ is the shear strength of the matrix and d is the diameter of the fiber. One half of the critical length is referred to as "transfer length".

If the actual length of the fibers is about ten times the critical length for example, the strength obtained with discontinuous fibers is found to be 95% that of continuous ones.

Davies[31] has reviewed the methods of preparation of composites and has concluded that an efficient means of making whisker-reinforced composites is by controlled eutectic or dendritic solidification. Ford[33] has examined the properties of an Al-Al$_3$Ni composite grown by unidirectional eutectic solidification. Transverse and longitudinal sections of the composite are shown in Figs. 12 and 13. The tensile strength of the chemically extracted Al$_3$Ni whiskers varied between 300,000 and 400,000 psi in tension and exhibited bending strengths as high as 800,000 psi. The tensile stress-strain properties of as-cast and of unidirectionally solidified eutectic Al-Al$_3$Ni specimens are shown in Fig. 14. A threefold increase in strength was observed for the unidirectionally solidified specimen over that solidified in the normal manner.

The technological value of whisker-metal matrix composites is yet to be established. However, the properties of room temperature fracture toughness and of elevated temperature strength are of special interest. The high fracture toughness of fiber reinforced composites appears to be due to one or more of the following factors: (1) a ductile matrix which can blunt the crack tip; (2) the deflection of the advancing crack by delamination of the composite; and (3) by the expenditure of large amounts of work in plastic deformation at the interface between the fiber and matrix.

With respect to elevated temperature properties, Sutton[34] reported that specimens of silver reinforced with whiskers of Al$_2$O$_3$ exhibited short

time (30 min.) tensile strengths of over 83,000 psi at 1600°F in air. In strength-to-weight ratio, this is equivalent to the best values of nickel or cobalt-base superalloys.

Solid Solutions

The strengthening effect of substitutional solute atoms in random solution is known to be small. The strengthening is caused by interaction between solute atoms and dislocations (see e.g. refs. 36,37). The simplest interaction is that due to size differences between solute atoms and solvent atoms. Edge dislocations would experience an attractive force from small atoms above its slip plane or a repulsive force from large atoms there. If the solute atoms have different moduli from the matrix atoms, there are further interactions. For example, dislocations would be repelled from regions of larger modulus and likewise the applied stress would have to be large enough to pull dislocations away from regions of lower modulus. In these cases the crystals can be imagined to contain "hard" and "soft" spots. The hardening in random substitutional solutions varies with concentration in a simple manner.[37] Dislocation locking can occur by atmosphere formation or by the Suzuki effect in close-packed metals.

The strongest solute atom-dislocation interactions occurs for asymmetrical distortions. Fleischer[36] has shown that large tetragonal distortions produce the strongest hardening, e.g. such as that found for interstitial elements in body centered structures. Experimental results have shown that the yield stress varies directly with the concentration or with square root of the concentration. For polycrystals, Nabarro[38] derived the

following expression:

$$\sigma_s \simeq G(E)^2 c \qquad\qquad (11)$$

where E is the misfit strain and c is the atomic fraction of solute. This law was observed to be obeyed by niobium containing interstitials[26] (see Fig. 3). For carbon in iron, E is approximately one-half, and the solubility limit of carbon in martensite is approximately 1.2 wt.% or about 5at.%. Thus from the above equation it would appear that the strengthening possible from the carbon in martensite should produce a yield strength of the order of $\frac{G}{80}$. This is about one-fifth of the theoretical strength and is a value very close to that observed in practice.

Non-Random Solutions

Appreciable hardening can also be obtained in substitutionally type solutions when the alloying elements are non-randomly distributed. In these cases there is not a simple dependence of yield strength on solute concentration.[39] Figure 15 shows the strengths obtained in a series of molybdenum-tantalum alloys in which "demixing" of the atoms occurs. The embrittlement of the concentrated alloys is thought to be associated with the large differences in elastic moduli between the two atom species. Solid solution systems in which the solute elements are not randomly distributed but yet are still in solution present a very interesting and potentially important class of materials. The ones that have been studied in greatest detail are those systems in which there is a miscibility gap in the solid state, so that under equilibrium conditions two solid solution phases co-exist. In such alloy systems, it is possible for the second phase to appear by the normal process of nucleation and growth of precipitated particles but, under certain conditions,

another reaction called "spinodal decomposition" may occur without the formation of nuclei of a second phase and without particles of a second phase appearing in the early stages of the transformation. One very interesting system exhibiting spinodal decomposition behavior is that of gold and platinum, the phase diagram for which is shown in Fig. 16. In this system, all phases have the same crystal structure, namely, face centered cubic. At a temperature where the two-phase field exists, the free energy, F, varies with the mole fraction of the dissolved element and, at one concentration, the second derivative of the free energy with respect to concentration is equal to zero. It is this criterion that determines whether or not a system will exhibit spinodal behavior. Although Cahn[40] and Hillert[41] have been actively exploring the theory of spinodal decomposition in alloy systems in recent years, the original concept goes back to Gibbs who classified decomposition reactions in solution systems into two categories; (1) in which the composition change was large and the volume very small, and (2) a change in which the composition fluctuation was very small but the volume over which it extended was very large. The first is a case of a normal nucleation and growth reaction; the second is that which has been called the spinodal. When a spinodal reaction occurs, atoms that are alike cluster and the distance between these clusters is very short, i.e. of the order of 20 to a few hundred atom distances. This clustering occurs spontaneously and simultaneously throughout the entire volume of the material, a condition unlike that of nucleation and growth where the nuclei are non-randomly located because they preferentially form at defects such as grain boundaries or dislocation networks within the crystal. Thus the spinodal reaction holds the promise

of providing the most uniform small-scale distribution of inhomogeneous regions of any reaction that is known at the present time. There is no doubt that the spinodal reaction produces a marked increase in the strength of the material as is shown in Fig. 17 which was taken from the work of Van der Toorn.[42] In this case, an 81% platinum-gold alloy was quenched from the single phase field and subsequently aged for various times, as indicated in the figure, at 600°C. The hardness increased from about 260 on the Vickers Microhardness scale to about 450 within a few minutes, and a high hardness was retained for many hours of aging thereafter. The exact processes whereby the spinodal reaction causes hardening are still under study and are not yet fully understood. Unfortunately, with alloy systems of this kind, even though the material is face centered cubic and one might expect it to be ductile, the materials quenched from high temperature and aged to produce the spinodal reaction have been found to be very brittle with failures occurring in tensile tests with elongations of less than 1%. The reasons for the brittle behavior are still unknown.

Ordered solid solutions or intermetallic compounds form another class of non-random solutions. Many ordered alloys work harder extremely rapidly but are relatively brittle[1] (e.g. Fe_3Si). The maximum effect is found in alloys that have an intermediate degree of order (see e.g. Westbrook[43]) and includes metals of widely different crystal structures. Alloys such as Fe_3Al which have relatively low values of the ordering energy do not show strong order dependent hardening. The theories of order hardening are plentiful but do not seem to be generally applicable, except perhaps for that due to Stoloff and Davies,[44] who considered the variation in spacing of the dislocation pairs making up the superlattice dislocation[7] with changing degree of order. The spacing in turn determines whether the partials

of the superdislocation glide independently or in pairs. If the dislocations
are coupled, order is perfectly restored and glide is easy. However, if the
partials glide as unit dislocations anti-phase boundary trails are created
behind each unit dislocation and hardening results. The actual domain size
in ordered alloys does not seem to control the strength.

Marcinkowski (private communication) has recently reported that the B2
type ordered alloys (e.g. FeAl, FeCo, FeRh) have two well-defined stages of
work hardening, a stage II which is temperature independent and with a
relatively high work hardening rate ($\sim G/100$) and almost linear, followed
by a temeprature dependent stage III, over which there is zero work hardening
and in which the stress level depends on the antiphase boundary energy.
Fe_3Si shows similar behavior except that the work hardening rate is greater
than that observed for B2 structures. Marcinkowski explains stage II in
terms of the accumulation of jogs on superlattice dislocations. Stage III
is interpreted in terms of thermally activated cross slip of screw dislocations.
Although these alloys are remarkably strong, they are unfortunately non-
ductile, (e.g. Fe-Rh shows a maximum breaking stress which is about 0.5 of
the theoretical but at strains of less than 1%), and unless means are
discovered to increase their ductility these ordered alloys are not of
much potential value.

A combination of heavily work-hardened, ordered structures is possible
by heat treatment. As mentioned earlier, the Cu-Al alloys (11-13% Al) undergo
a phase transformation to martensite resulting in a complex superlattice
that is heavily faulted. If the martensite is aged to increase the degree
of order, nearly a two-fold hardening occurs. Whether such effects can be
utilized for obtaining high strength ductile alloys remains to be seen.

In short range ordering, dislocations have to overcome local solute atom
barriers. Unit dislocations can disorder or re-order the structure,

leading to expenditure of energy. In either case the applied stress has to do the necessary work. Local elastic interactions when the moduli differ widely may also lead to hardening.[39] Similar effects may occur in clustered solid solutions.[36,37]

SOME EXAMPLES OF USEFUL HIGH-STRENGTH SYSTEMS

An interesting example of the effect of hard dispersed particles on the dislocation network resulting from plastic deformation is that provided by TD nickel (in which thoria particles are dispersed). Figures 4 and 9 show a comparison between the substructures produced in high-purity nickel and in TD nickel.[28] The cell size in the TD nickel is about half that found in the high-purity material. The fact that the particles in this case are refractory, and are substantially insoluble in the nickel, also has a beneficial effect on the high temperature strength. This dispersed phase does not dissolve or coalesce at high temperatures and thus stabilizes dislocation networks at elevated temperatures. The particles impede climb as well as glide of dislocations. The result is that the material retains high strength even at elevated temperatures. The dislocation networks are so effectively pinned by the thoria in the TD nickel that it is extremely difficult to re-crystallize this material even at temperatures near the melting point.

Because of the relatively low cost and large usage of ferrous materials, more effort has been devoted to determine strengthening processes in steels than in any other metal. As was shown in Fig. 1, some ferrous alloys already have been produced with strengths in excess of 500,000 psi.[45] Such high strengths, however, cannot be produced by simple one-step processes. Ausforming, a relatively new process used for producing high strengths in steel, combines the effects of cold work and precipitation with a phase change. It has been shown that the deformation of metastable austenite prior to its transformation

into martensite produces a large volume fraction of finely dispersed
alloy carbides which do not grow much upon tempering the subsequently
formed martensite until high tempering temperatures (>500°C) are used.[29]
Such particles increase the rate of multiplication of dislocations so that
very high densities of dislocations are produced in the deformed material
(estimated to be about $10^{13}/cm^2$). Figures 18a, b are electron micrographs
showing the heavily deformed structure and the dispersed carbides. Once
deformed, the austenite is quenched to produce martensite; the martensitic
structure thus produced is very much finer than that produced by a direct
quench from the austenite range without the intermediate plastic
deformation. Furthermore, the martensite transformation itself is a source
of dislocation generation and this contributes to the total number of
dislocations present in the ausformed steel. The resulting structure is
extremely complex as Fig. 18 shows. The high strength of ausformed steels
can be accounted for by the high dislocation density and by the fact that
these dislocations are pinned by finely dispersed precipitated particles
of alloy carbides.[29]

Another series of promising dispersion strengthened alloys are the
maraging steels based on a high nickel content combined with several other
alloying elements in smaller amounts, but with no appreciable carbon (i.e.
carbides are not utilized as in the other high strength steels). Ordering
may also contribute to the strength of these materials. Structure-property
correlations are needed so that the strengthening mechanisms can be more
completely understood and in order to utilize the materials to their maximum
capability. Although the maraging steels are not as strong as the ausformed
steels, ausforming of maraging alloys has been successful in further increasing
their strength.[46]

A SUMMARY OF THE PRESENT SITUATION

Table IV indicates some of the methods by which alloys can be strengthened. To achieve the maximum strength, a high dislocation density is required and thermal-mechanical, rather than simple heat treatment, provides the best combination of strength and ductility.

Figure 19 shows the ratio of the measured to the theoretical strength for alloys of several metals. The absicissa in this figure is the equivalent temperatire (in ^{o}K) which is the test temperature divided by the temperature at the melting point of the metal. The effects of the concerted efforts of research and development on steels and on aluminum and titanium alloys is evident in the figure. It can also be seen that the present stage of alloy development for the refractory metals is in its elementary stages. Significant improvements in the strengths of refractory alloys are certainly possible and can well result from additional research and development work on these materials. Beryllium is a metal that appears to be very attractive. It has low density, a high modulus, and potentially high strength. However, it crystallizes in the hexagonal close-packed structure and is very brittle at ordinary temperatures. One of the problems associated with brittleness in hcp systems is that the critical resolved shear stress is often too high for all the necessary slip systems to operate.[47] Attempts must be made to impart ductility to beryllium, e.g. by alloying to obtain the cubic structure. However, besides the brittleness of beryllium that precludes its use, beryllium alloys in usable form are very expensive, with costs ranging up to $100 or more per pound.

Even though high strength, ductile steels are available, additional improvements are possible and desirable. Encouraging results have been obtained with certain alloys by quenching and tempering in repeated cycles as illustrated in Fig. 20. These treatments are effective in producing

fine grained martensite without the complications of hot forming as is necessary for the ausforming process. Yield strengths have been improved by as such as 50% over those produced by conventional heat treatments by such cycling operations. Additional improvements in properties have been obtained by combining ausforming with elevated temperature strain aging as is illustrated in Fig. 21. It is worthy of note that elevated temperature strain aging does not necessarily reduce the ductility of ausformed steels.

One of the most interesting potential areas of investigation is that of the "spinodal" alloys in which high strength can be produced in two-phase solid solution alloy systems. In all cases investigated to date, however, even though the strength levels obtained in such materials were high, the alloys have been brittle and hence of limited interest or use. Additional investigations, particularly of structure, are needed to reveal the cause of the brittle behavior of these materials.

In conclusion, it should be recognized that while a great deal of progress has been made in producing high strength materials, there is a great deal yet to be done combining high strength with high toughness.

ACKNOWLEDGMENT

Table I

Some Representative Metal Wire, Whisker and Fiber Strengths*

Material	Tensile Strength (in units of 10^6 psi)	Young's Modulus (in units of 10^6 psi)	Strength-to-Weight Ratio (Tensile Strength/Density, in units of 10^5 inches)	Melting Point (°C)
Metal Wires**				
Carbon steel (0.90C)	0.575	30	0.7	1450
Stainless steel	0.347	29	0.44	1425
Mo	0.300	53	0.29	2610
Be	0.160	45	0.89	1284
Glass, Ceramics & Polymers				
Asbestos	0.85	27	3.4	Dehydrates at 500
Mica	0.45	33	1.67	Dehydrates between 350 and 700
Drawn Silica	0.86	10.5	3.5	1700
Glass in air	1.50	10.5	6.0	-----
Solution Spun Nylon 4	0.27	-----	2.4	-----
Whiskers				
Graphite	2.8	98	12.7	3000 (sublimes)
Al_2O_3	2.2	76	5.5	2050
Fe	1.8	28	2.3	1540
SiC	3	100	31	2600

* Taken from the work of Davies[31]

** All wires 0.006 inches in diameter except Be which is 0.070 inches in diameter.

Table II

Material	Shear Modulus[1] G. psi	Density P lb/cm^3	Theoretical Ratio G/P	Theoretical tensile[2] yield 0.15G (psi)	Max. Observed tensile strength (psi)	Ratio $\frac{Obs.}{Theor.}$
Al (fcc)	4 X 10^6	0.16	4 x 10^7	600,000	100,000 (alloy)	0.17
Pb (fcc)	7 X 10^5	0.41	1.8 X 10^6	100,000	12,000 (alloy)	0.12
Cu (Fcc)	5 X 10^6	0.32	1.5 X 10^6	750,000	214,000 (alloy)	0.35
Be (hcp)	16 X 10^6	0.07	2 X 10^8	2,400,000	80,000	0.03[5]
Mo (bcc)	16 X 10^6	0.37	4.3 X 10^7	2,400,000	80,000 (alloy)	0.03[5]
W (bcc)	27 X 10^6	0.70	3.8 X 10^7	4,000,000	300,000 (alloy)[3]	0.075[5]
Nb (bcc)	5.3 X 10^6	0.31	1.7 X 10^7	800,000	110,000 (alloy)[4]	0.14
Fe (bcc)	12 X 10^6	0.38	4.3 X 10^7	1,800,000	1,000,000 (whiskers)	0.56
					500,000 (ausformed alloys)	0.3
					700,000 (drawn wire)	0.4

Notes: (1) Data from Metals Handbook (ASM) or assumed 0.38E.

(2) Calculated on basis of G for pure metal — for alloys theoretical may be different because G may be changed by alloying.

(3) W-Ta-Mo alloys.

(4) Nb – 11W – 28Ta 2r (alloy FS 85, Fansteel).

(5) Limited data available.

Table III

Treatment	Hardness (VPN)	C Cell Size (statistical mean)
70Kb	125	0.53μ
130Kb	160	0.32μ
250Kb	190	0.17μ

Table IV

Dispersions	Characteristics	Methods of Producing
Ductile	Low to moderate strength, good ductility	Age-hardening (Al alloys alloy steels)
Spinodals	High strength possible but poor ductility common	Heat treatment as for age-hardening
Refractory	Very high strengths possible with poor or moderate ductility	Compacting, powder metallurgy as in Ni and W base alloys. Special processes, e.g. Dupont TD Ni. Internal oxidation of an alloy so as to cause one component to precipitate as an oxide. Fiber techniques. Eutectic alloys. Combination of thermal-mechanical treatments, e. g. strain aging, ausforming.

REFERENCES

1. The Strengthening of Metals. Ed. D. Peckner (Reinhold Publishing Co.), 1964.

2. High Strength Materials. Ed. V. F. Zackay (J. Wiley & Sons, New York), 1965.

3. A. H. Cottrell, Dislocations and Plastic Flow in Crystals (Oxford, Clarendon Press), 1953.

4. A. H. Cottrell, Theory of Crystal Dislocations (Gordon-Breach), 1962.

5. Fracture of Solids. Eds. D. C. Drucker and J. J. Gilman (Interscience, New York), 1963.

6. E. Orowan Symposium on Internal Stresses in Metals and Alloys, Inst. Metals (London) p. 451, 1948.

7. Electron Microscopy and Strength of Crystals. Eds. G. Thomas and J. Washburn (Wiley & Sons, New York), 1963.

8. J. Friedel, Dislocations (Addison-Wesley), 1964, see also ref. 2 p. 154.

9. W. G. Johnston and J. J. Gilman, J. Appl. Phys., 30, 129 (1959).

10. G. Hahn, R. Reid and A. Gilbert, "Symposium on the Role of Substructure on Mechanical Behavior of Metals", ASD-TOR-63-324 p. 253 (1963).

11. A. H. Cottrell, Relation of Structure and Mechanical Properties of Metals (H. M. S. O. London), p. 455, 1963.

12. R. W. K. Honeycombe, H. J. Harding, and J. J. Irani, ref. 2, p. 213.

13. Symposium on Relation of Structure and Mechanical Properties of Metals (H. M. S. O. London), 1963.

14. H. Wildersich, AIME J. Met., 16, 425 (1964).

15. H. Conrad, ref. 2, p. 436.

16. A. Kelly and R. B. Nicholson, Prog. Mat. Sci. 10, 149 (1963).

17. G. Thomas, AIME J. Met. 16, 365 (1964).

18. A. Berghezan and A. Fourdeux, "Symposium on the Role of Substructure on Mechanical Properties of Metals", ASD-TOR-63-324 p. 437 (1963).

19. W. J. Petch, J. Iron Steel Inst. 174, 25 (1953).

20. E. O. Hall, Proc. Phys. Soc. 64B, 747 (1951).

21. A. K. Mukherjee, J. D. M te and J. E. Dorn, Trans. AIME (in press) UCRL-11888.

22. G. Saada, ref. 7, p. 651.

23. D. H. Warrington, Proc. European Conf. Electron Microscopy, Delft, Holland. p. 354 (1961).

24. R. L. Nolder and G. Thomas, Acta Met., 12, 227 (1964).

25. W. C. Leslie, D. W. Stevens and M. Cohen, ref. 2, p. 382.

26. L. I. van Torne and G. Thomas, Acta Met. 11, 881 (1963).

27. J. B. Mitchell, S. K. Mitra and J. E. Dorn, Trans. ASM, 56, 236 (1963).

28. M. von Heimendahl and G. Thomas, Trans. AIME 230, 1520 (1964).

29. G. Thomas, D. Schmatz and W. Gerberich, ref. 2, p. 251.

30. A. Kelly and W. R. Tyson, ref. 2, p. 578.

31. G. L. Davies, ref. 2, p. 603.

32. A. Kelly and G. L. Davies, Metallurgical Reviews, Vol. 10, 37 (1965), p. 1-77.

33. J. A. Ford, ref. 2, p. 638.

34. W. H. Sutton, ref. 2, p. 599.

35. J. Peterson, ref. 2, p. 380.

36. R. L. Fleischer, ref. 1, p. 93.

37. R. L. Fleischer and W. R. Hibbard, ref. 13, p. 261.

38. F. R. N. Nabarro, "Report of Conf. on Strength of Solids", Phys. Soc. London, p. 38, 1948.

39. L. I. van Torne and G. Thomas, Acta Met. (to be published).

40. J. W. Cahn, Acta Met., (9), 795-801 (1961).

41. M. Hillert, Acta Met. (9), 525-535 (1961).

42. L. J. van der Toorn, Acta Met., 8, 715 (1960).

43. J. H. Westbrook, ref. 2, p. 724.

44. N. S. Stoloff and R. G. Davies, Acta Met., 12, 473 (1964).

45. D. Schmatz, F. Schaller and V. F. Zackay, ref. 13, p. 613.

46. R. H. Bush, Trans. AIME, 56, 885 (1963).

47. J. E. Dorn and J. B. Mitchell, ref. 2, p. 510.

FIGURE CAPTIONS

1. A plot of the tensile yield strength versus barrier separation predicted from the simple Orowan yield theory. The theoretical maximum is indicated at 0.15G.

2. Schematic stress-strain curves illustrating differences in yield behavior of impure bcc metals and fcc metals. The Luders strain is indicated by the region B. Work hardening occurs over the region C. The effect of barriers is to raise the yield point and the work hardening rate.

3. Experimental data showing the effect of impurity and grain size on mechanical properties of niobium. The total impurity contents in atom fractions are: A. 2.6×10^{-3}, B. 3.8×10^{-3}, C. 5.3×10^{-3}, D. 6.5×10^{-3}, E. 1.5×10^{-3}. Work hardening of specimen B is more rapid because impurities have precipitated out leading to more rapid dislocation multiplication. (Courtesy Acta Met., ref. 26).

4. Dislocation cell structure in polycrystalline nickel, tensile deformed 20% at 295°K. (Courtesy Acta Met., ref. 24).

5. Experimental data of Mukherjee et al. (ref. 21) showing the increase in work hardening rate with increasing number of operative slip systems. The crystal orientations and operative slip systems are indicated on each curve.

6. The experimental data of Warrington (ref. 23) relating the flow stress of copper to the cell diameter. Extrapolation to the theoretical strength limit predicts a cell size of 0.12μ.

7. Electron micrographs showing dislocation substructures produced after explosive deformation: a) 70 kb, b) 130 kb, c) 250 kb. (Courtesy Acta Met., ref. 24).

8. Scheme illustrating how dispersed particles can act as dislocation multiplication centers by causing cross slip.

9. (a) Substructure in TD nickel after 90% cold rolling of extruded bar. (b) Stress-strain properties of TD-nickel compared to pure nickel. Annealing treatments after 90% cold rolling of extruded stock. (Courtesy Trans. AIME, ref. 28).

10. Schematic stress-strain curves illustrating the effect of barriers on the hardening rate of metals. Compare to Fig. 3.

11. The stress-strain curves of tungsten wire, bulk copper, and two tungsten wire-copper composites of varying volume fractions of fibers. (Courtesy Inst. Metals, London, ref. 32).

Figure Captions (continued)

12. Transverse section of Al-Al$_3$Ni eutectic unidirectionally
    solidified at 0.66 cm/hr. (Courtesy J. Wiley and Sons,
    ref. 33).

13. Longitudinal section of same alloy shown in Fig. 12 but
    after solidification rate of 8.5 cm/hr. (Courtesy of
    J. Wiley and Sons, ref. 33).

14. The tensile-stress-strain properties of as-cast and of
    unidirectionally solidified eutectic Al-Al$_3$Ni specimens.
    (Courtesy J. Wiley and Sons, ref. 33).

15. Showing the marked solid solution hardening obtained in Ta-Mo
    alloys which become non-random for concentrations greater than
    about 20% solute.

16. The phase diagram for Au-Pt alloys.

17. Age hardening response of spinodally decomposed Au-Pt alloys.
    (Courtesy Acta Met., ref. 42).

18. (a) Retained austenite and martensite in Fe/16 Ni/0.3C/4.7Cr
    steel ausformed 30% at 500°C and quenched. (b) Dark field
    electron micrograph showing small particles (50-150A diam.)
    of VC in martensite produced by ausforming Fe/25 Ni/0.3C/1.9V
    steel 30% at 500°C. (Courtesy O. Johari).

19. Maximum measured tensile strength divided by the theoretical
    strength shown as a function of equivalent temperature for
    several metals. (Courtesy J. Wiley and Sons).

20. (a) Scheme illustrating the process for hardening by cyclic
    transformation of austenite. The associated expected micro-
    structures at the different stages are shown. (b) Variation
    of hardness with quenching temperature for several levels of
    cold working for steel. Each cycle is followed by tempering
    at 914°F for 10 minutes. (Courtesy J. Wiley and Sons).

21. Stress-strain curves of ausformed H-11 steel in the quenched
    and tempered condition (left diagram) and in the quenched
    tempered and elevated temperature strain-aged condition
    (right diagram). (Courtesy of J. Wiley and Sons.)
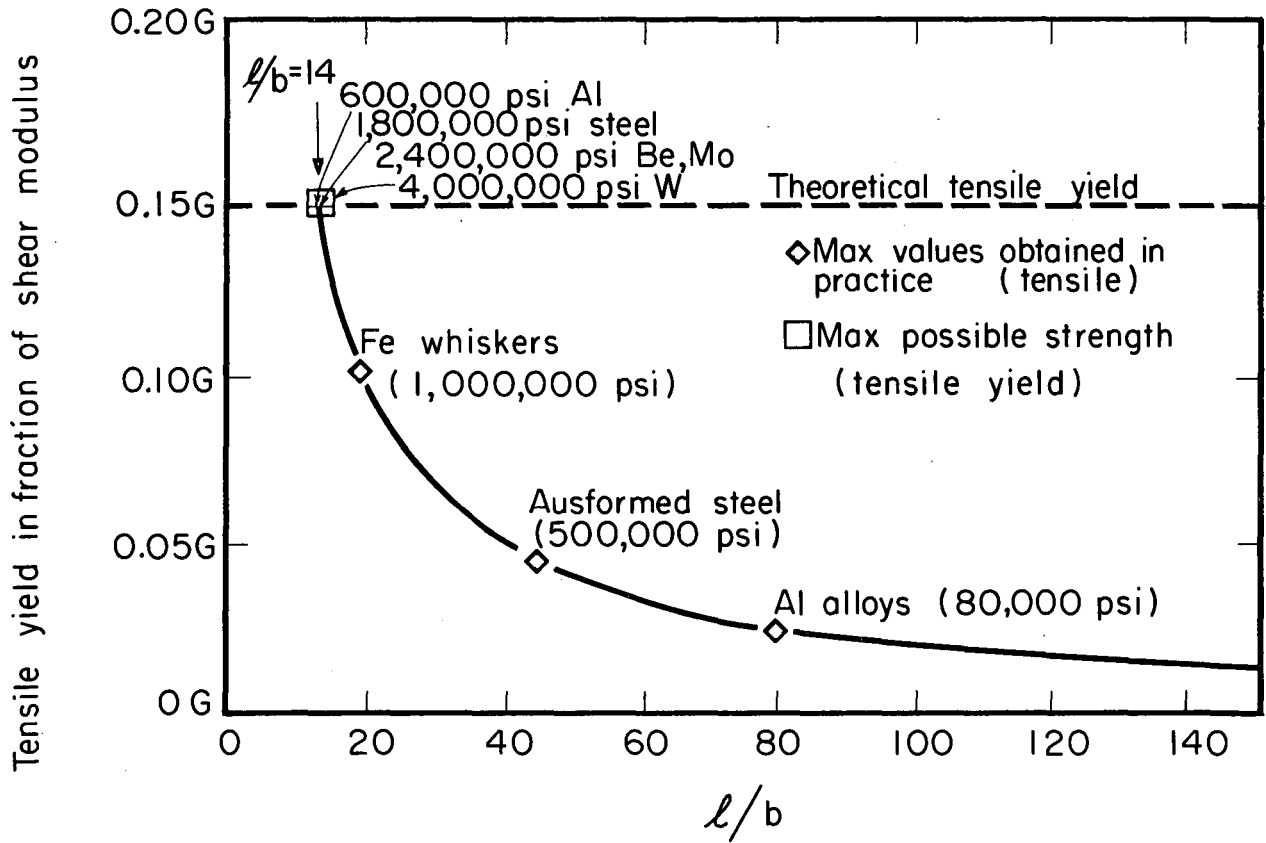
MUB-6755

Fig. 1

MUB-6754

Fig. 2

Fig. 3

MU-27850

ZN-3764

Fig. 4

Fig. 5

MUB-6750

MUB-6753

Fig. 6

(a)   (b)   (c)

0.5 µ   0.5 µ   0.5 µ
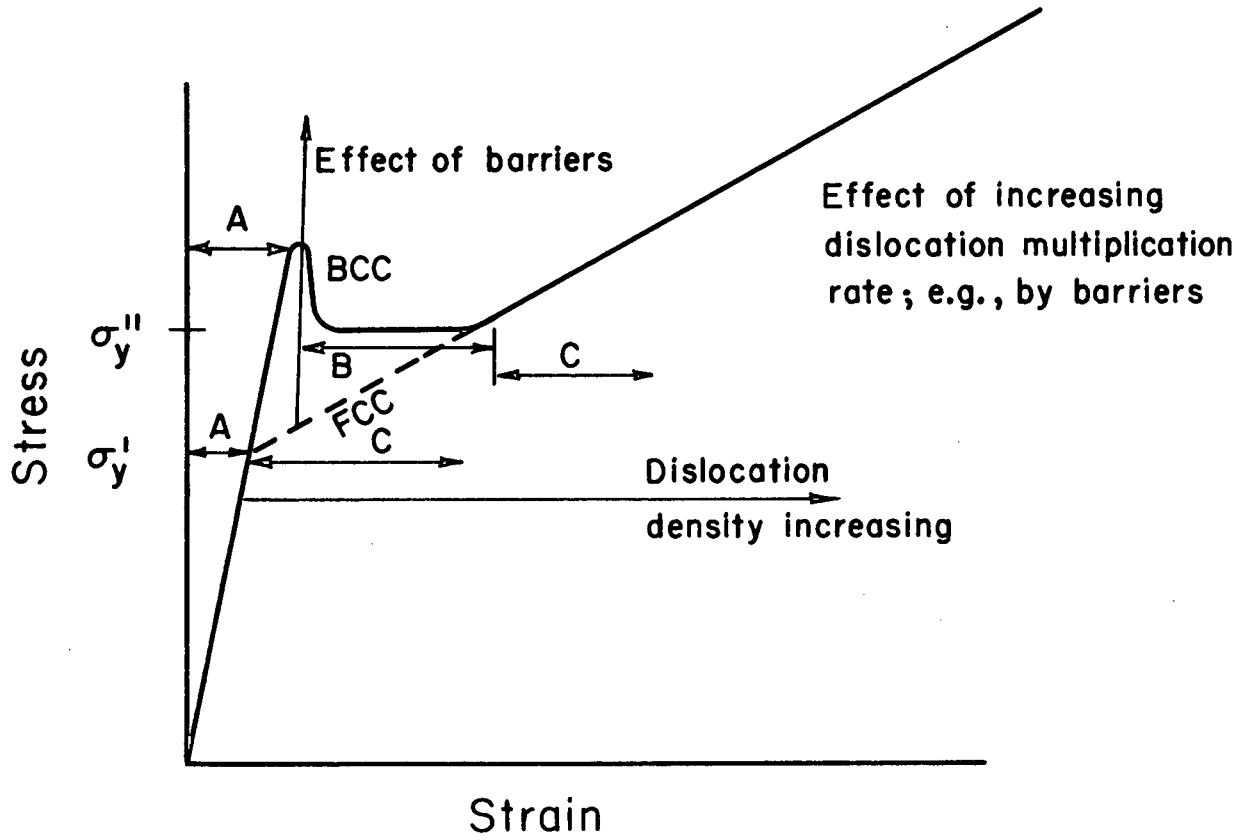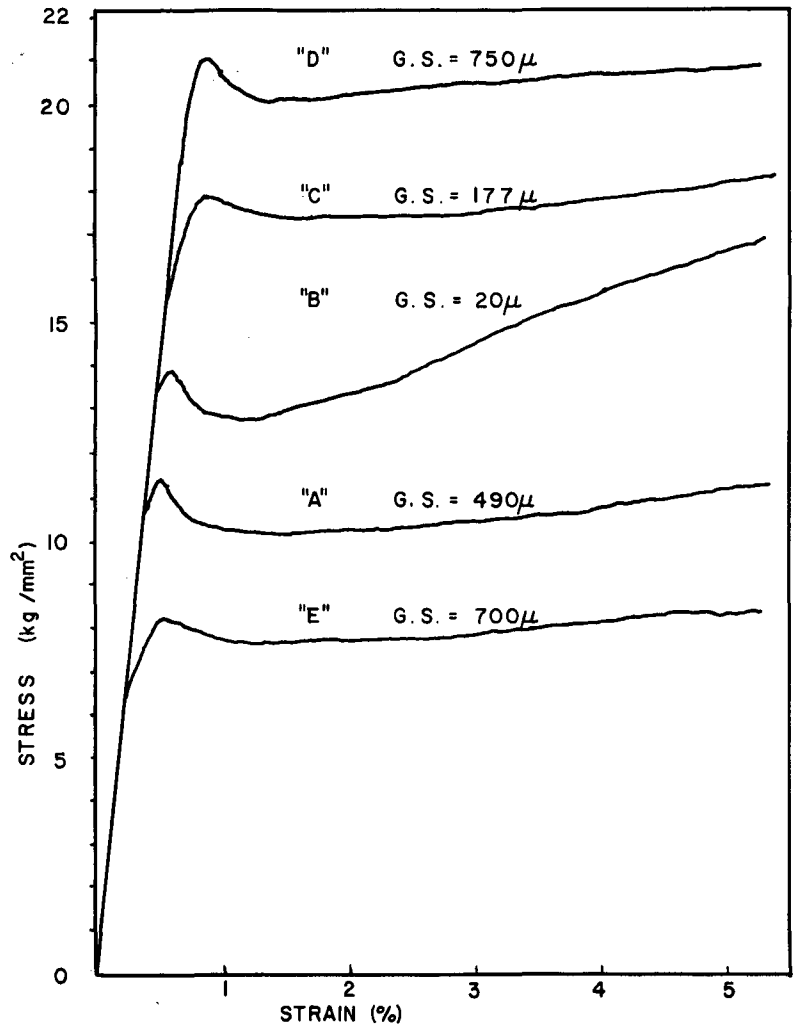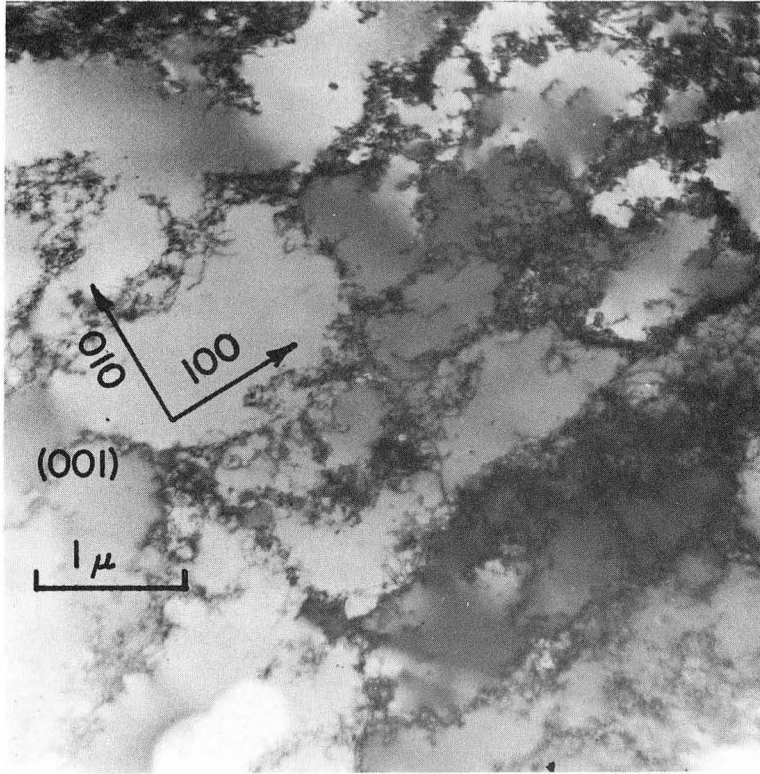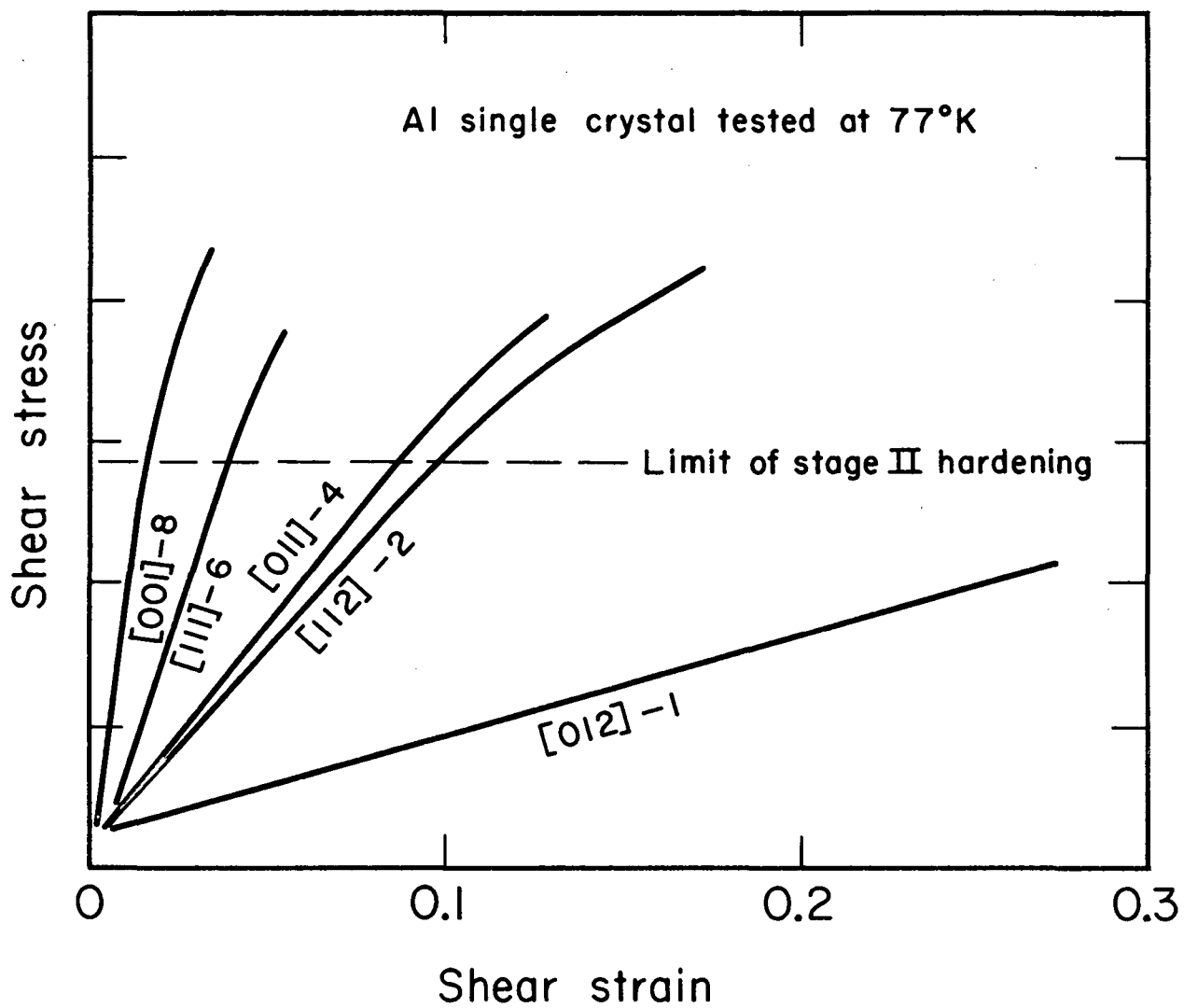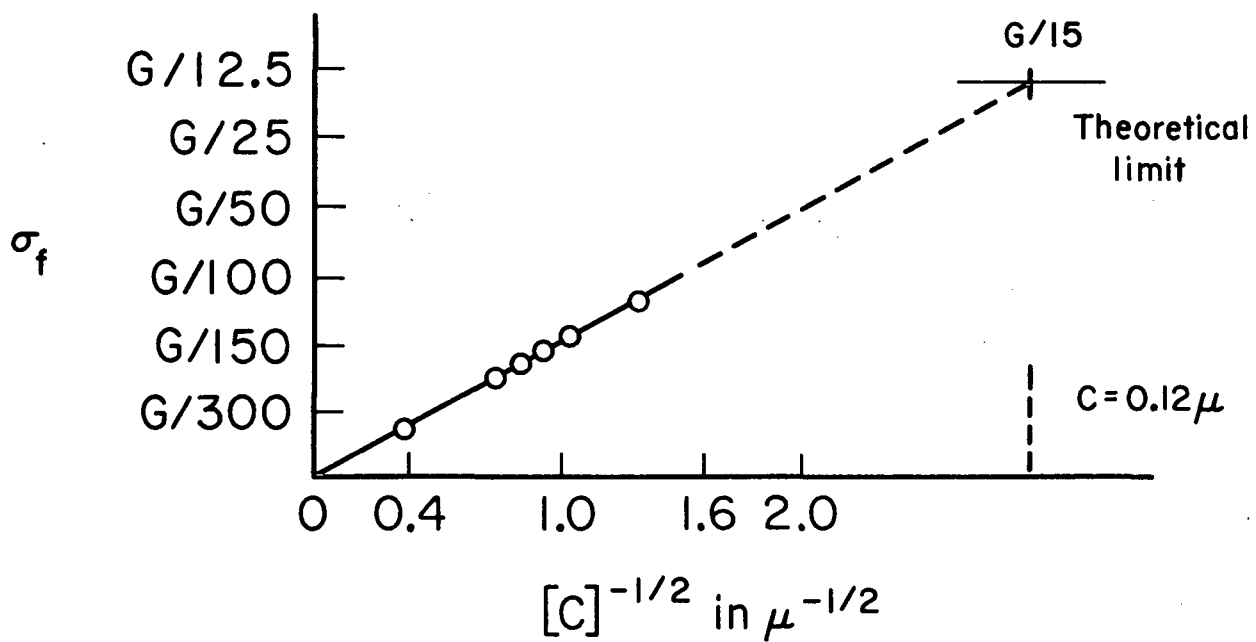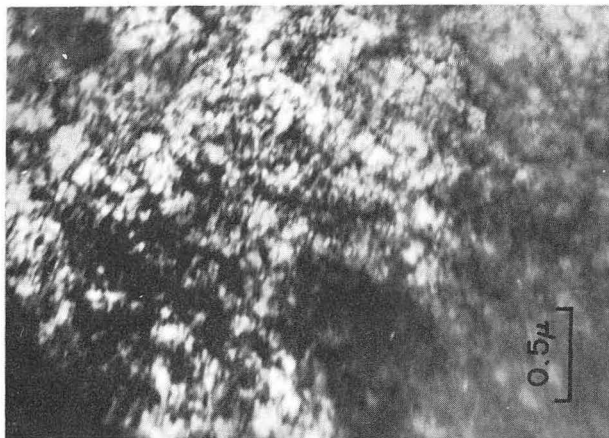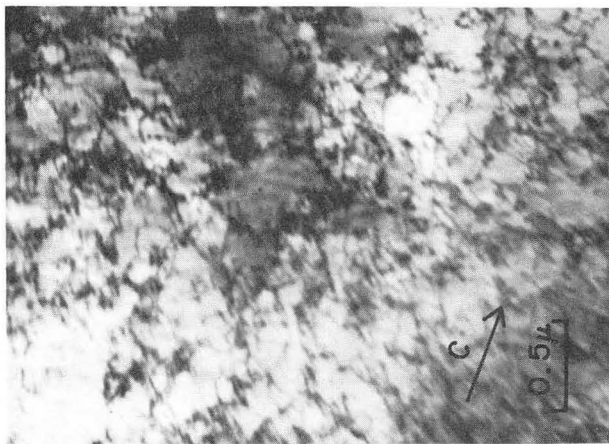
C   C

ZN-3785

Fig. 7
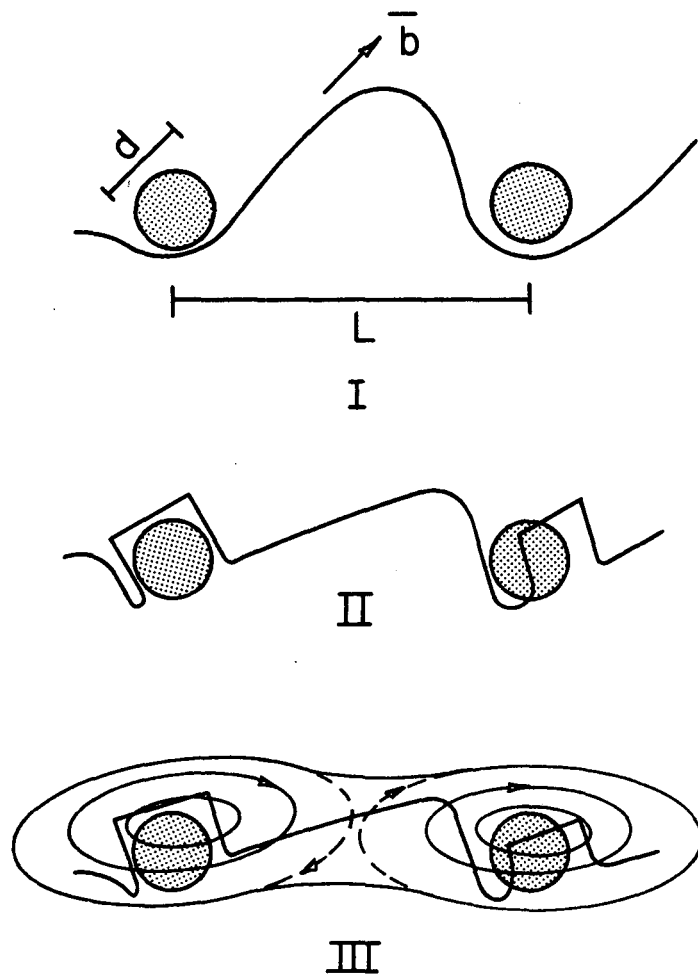
MU-36191

Fig. 8
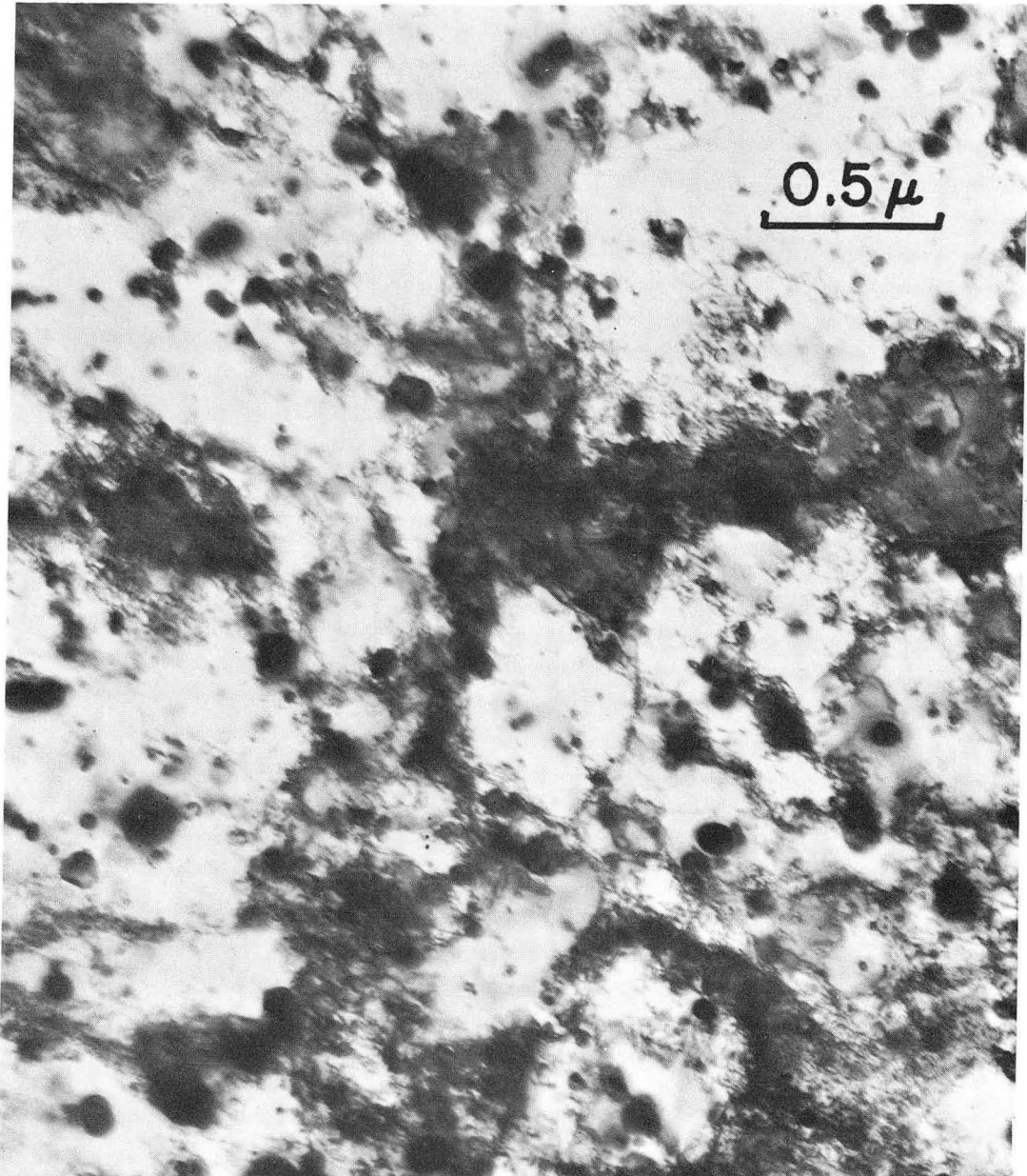
Fig. 9a
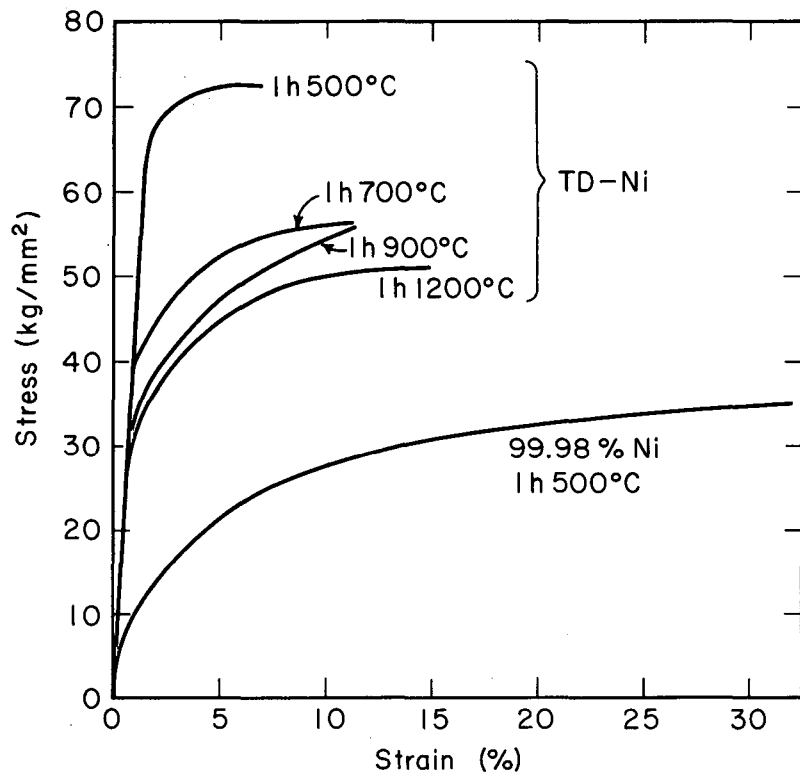
MU-33302

Fig. 9b
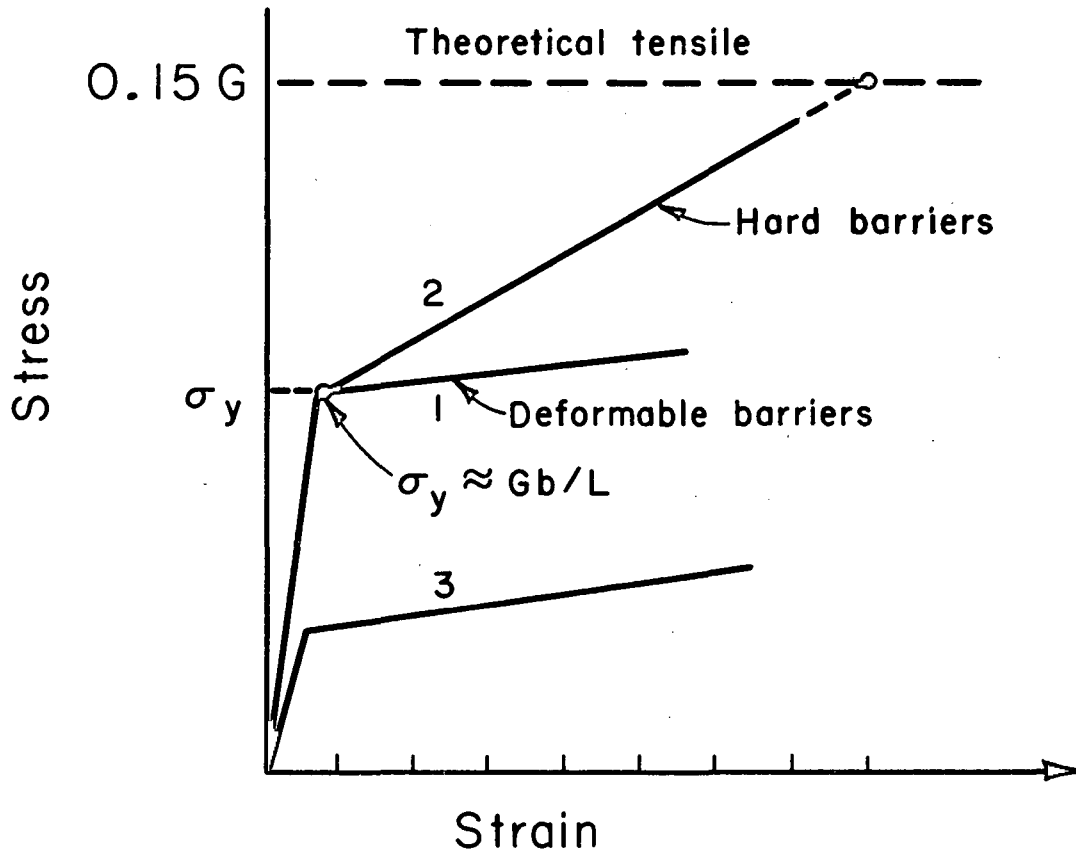
Fig. 10
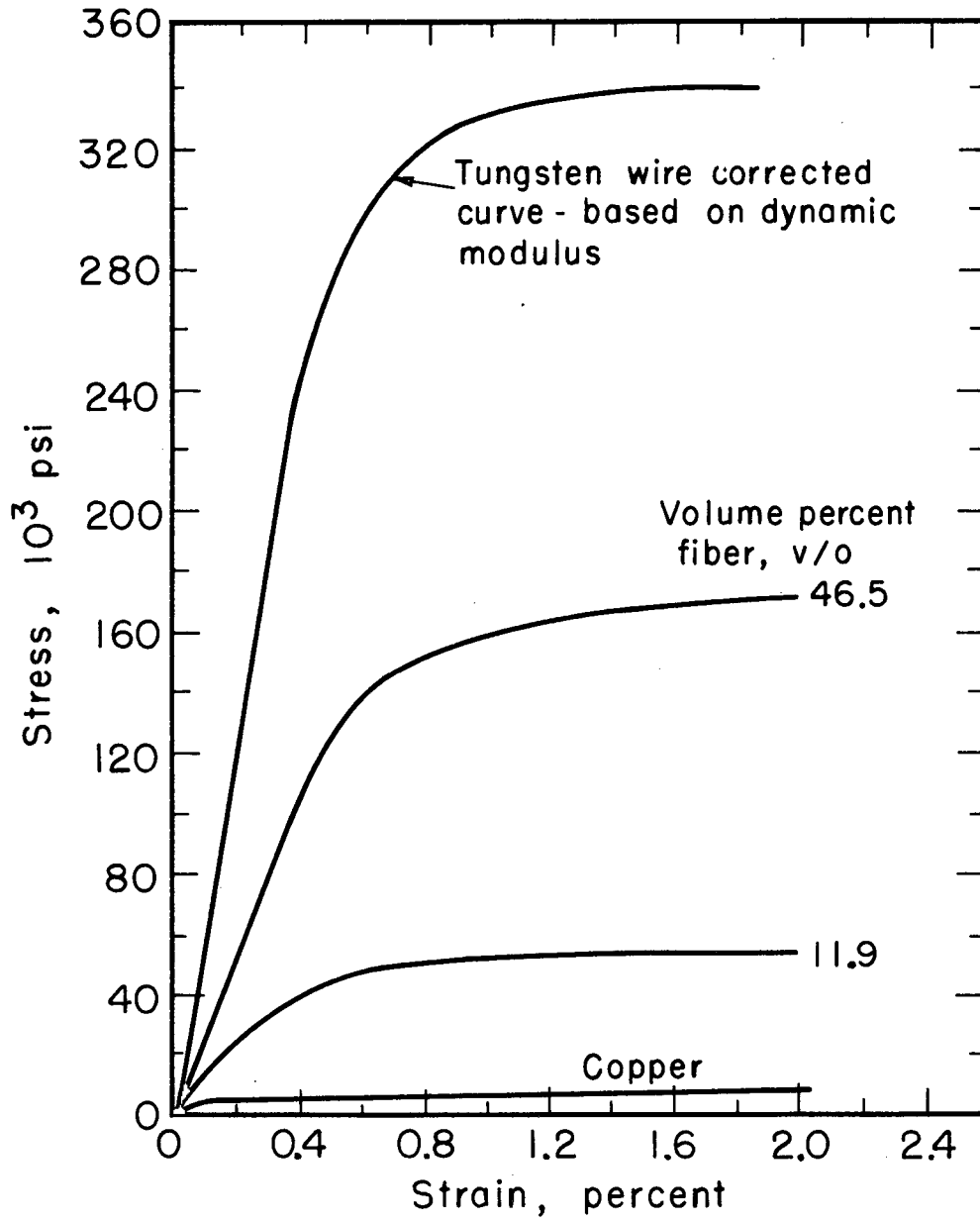
MUB-6751

Fig. 11

MUB-7300
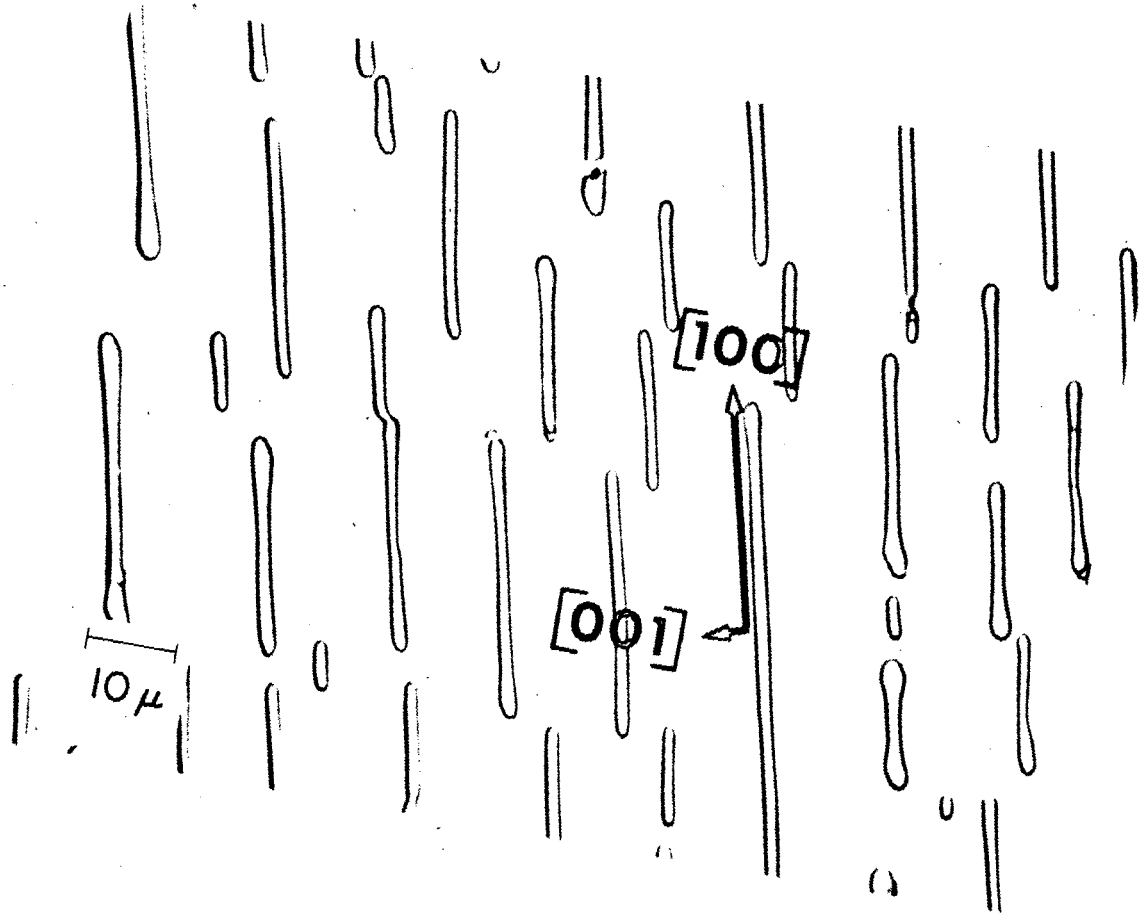
Fig. 12
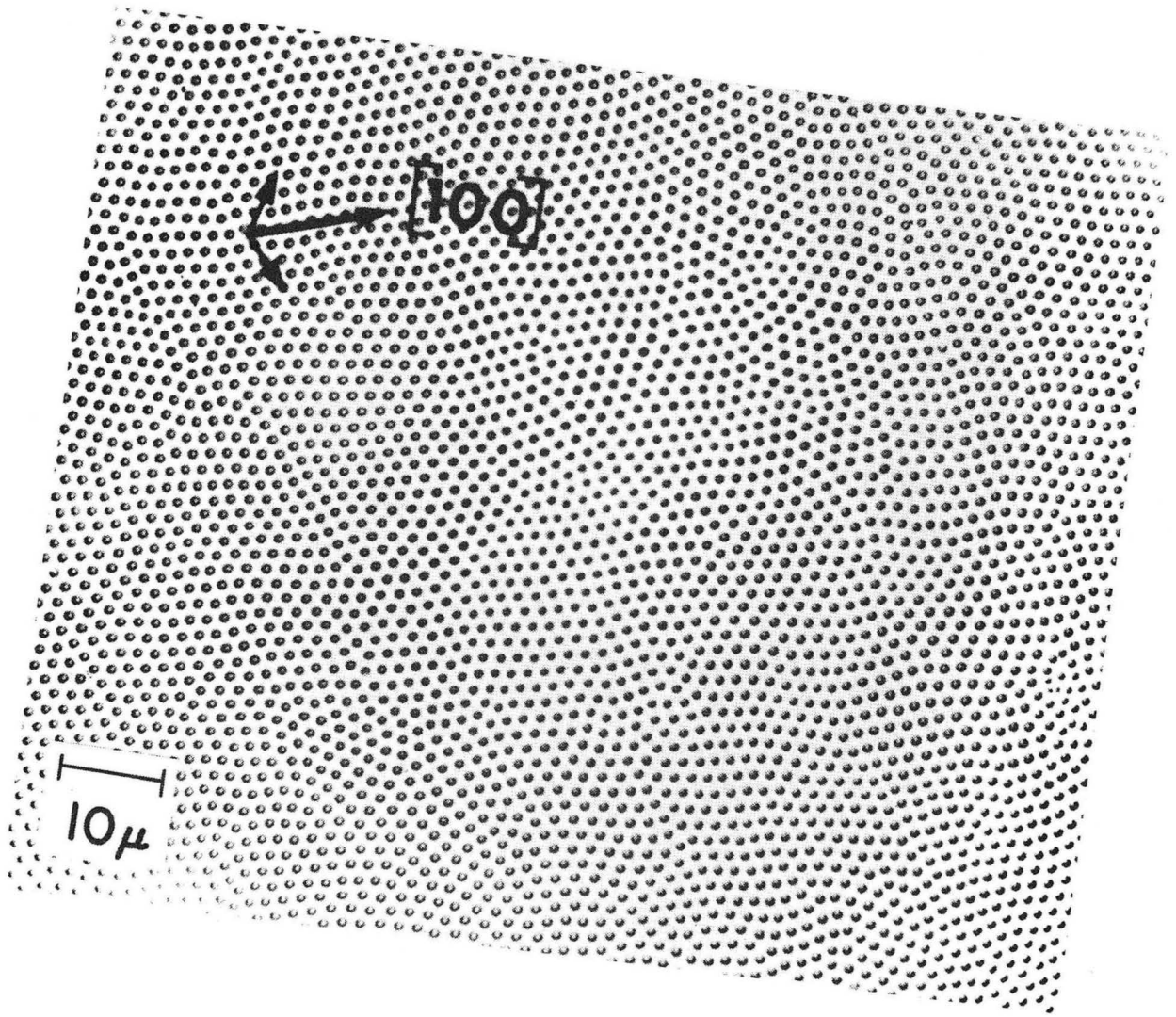
MU-36772

ZN-5182

Fig. 13

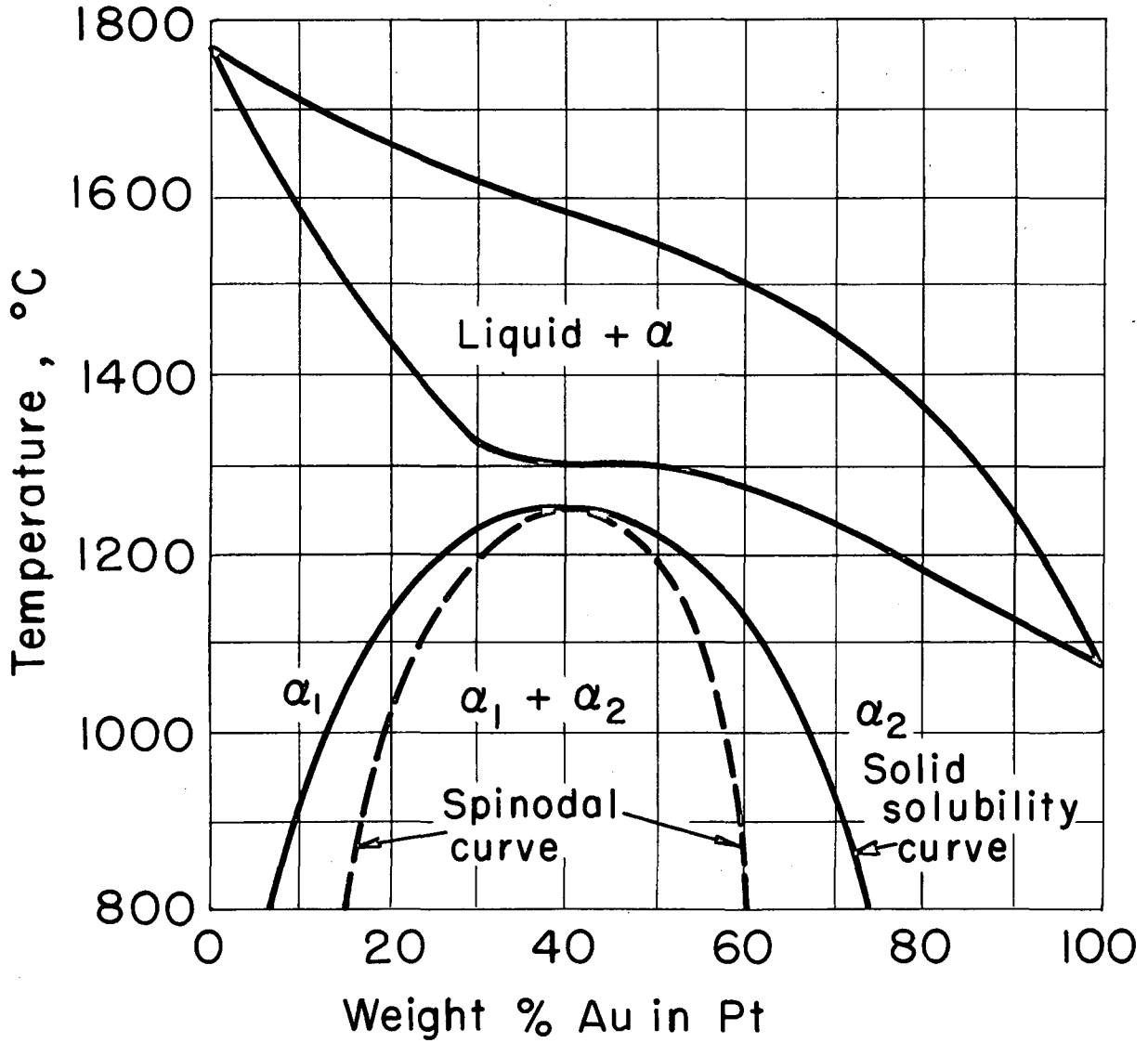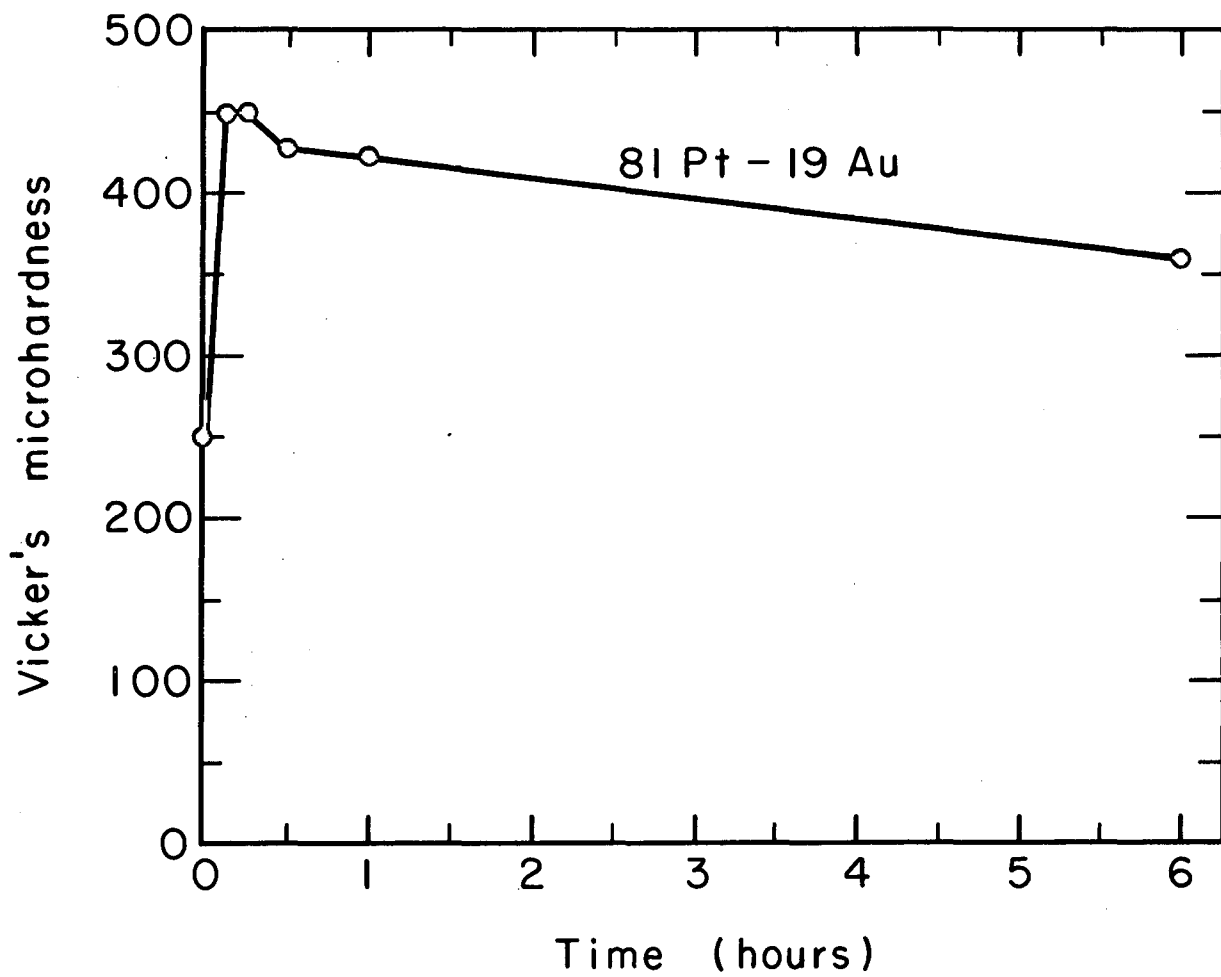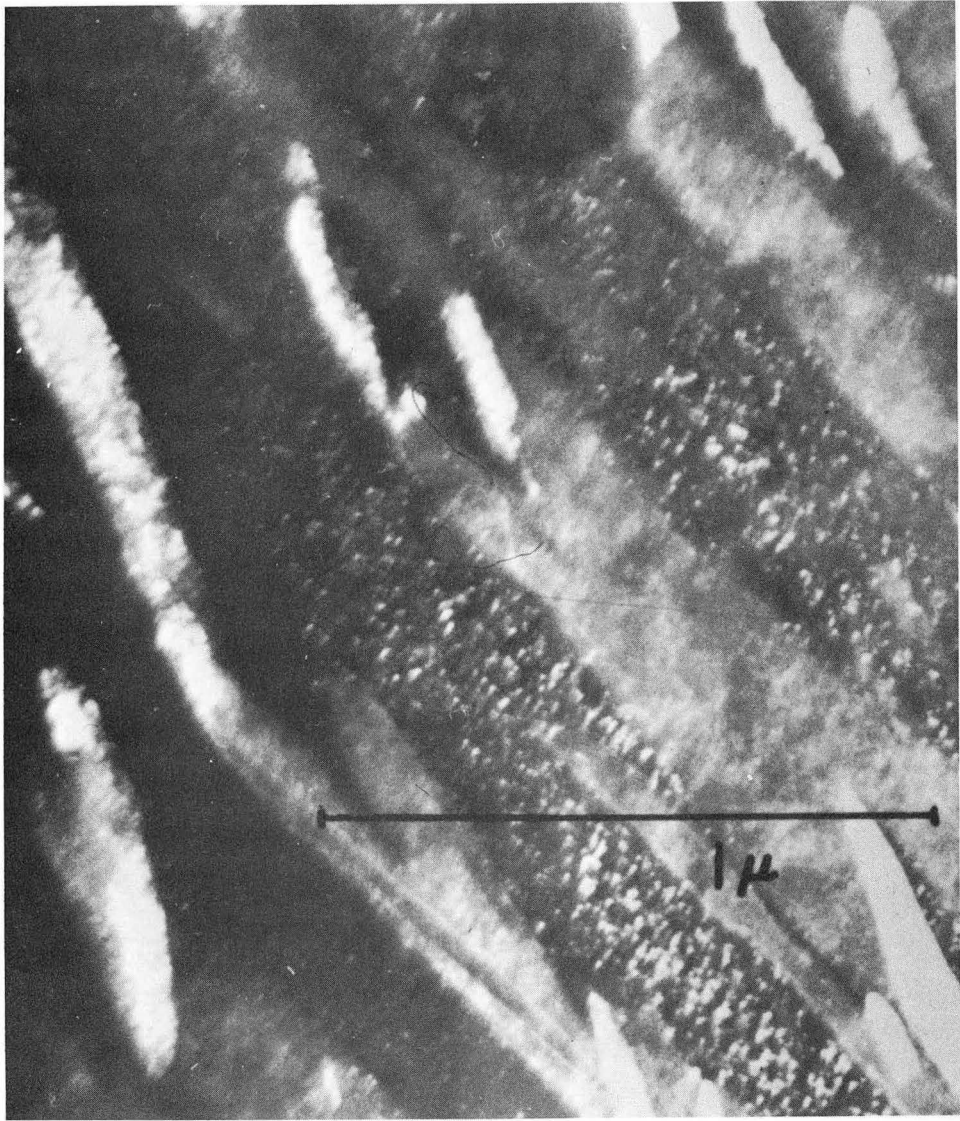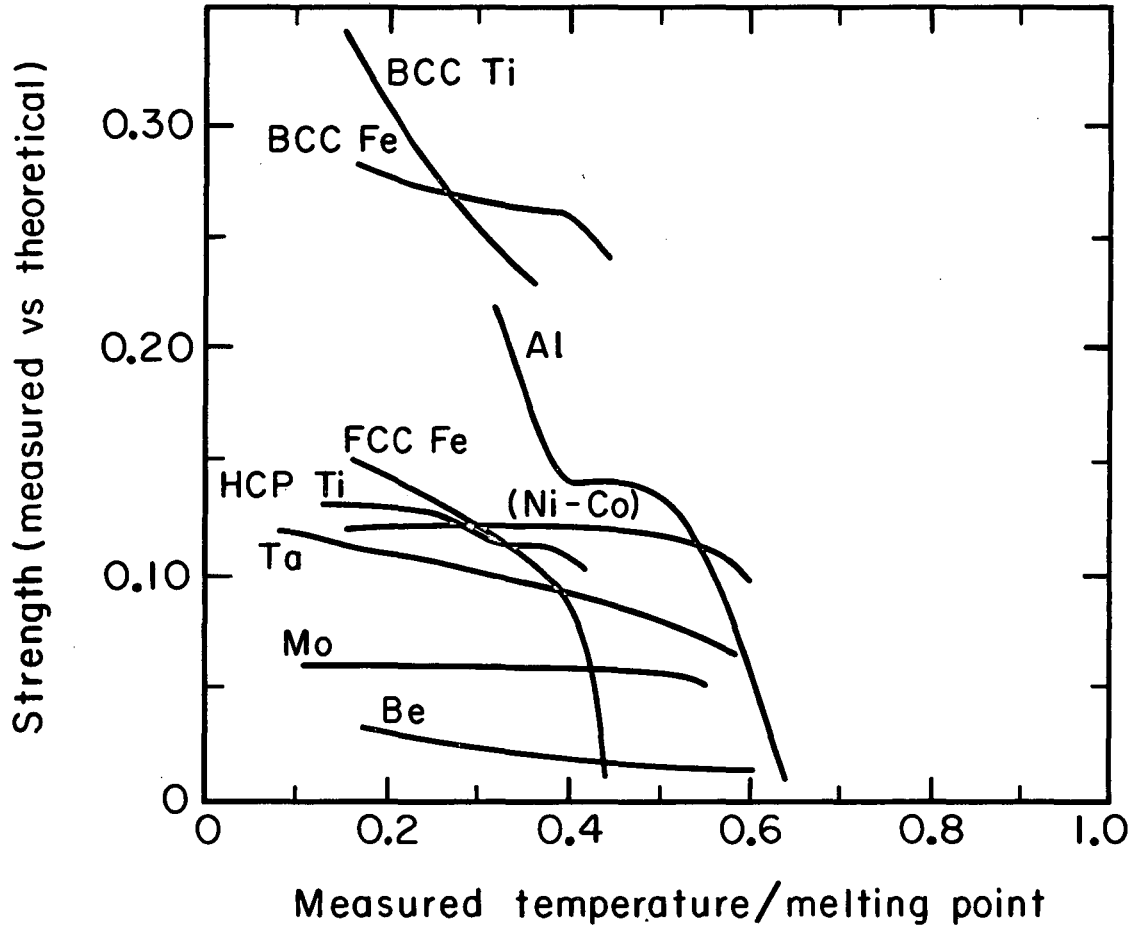MU-36771

Fig. 14

Fig. 15

MUB-6752

Fig. 16
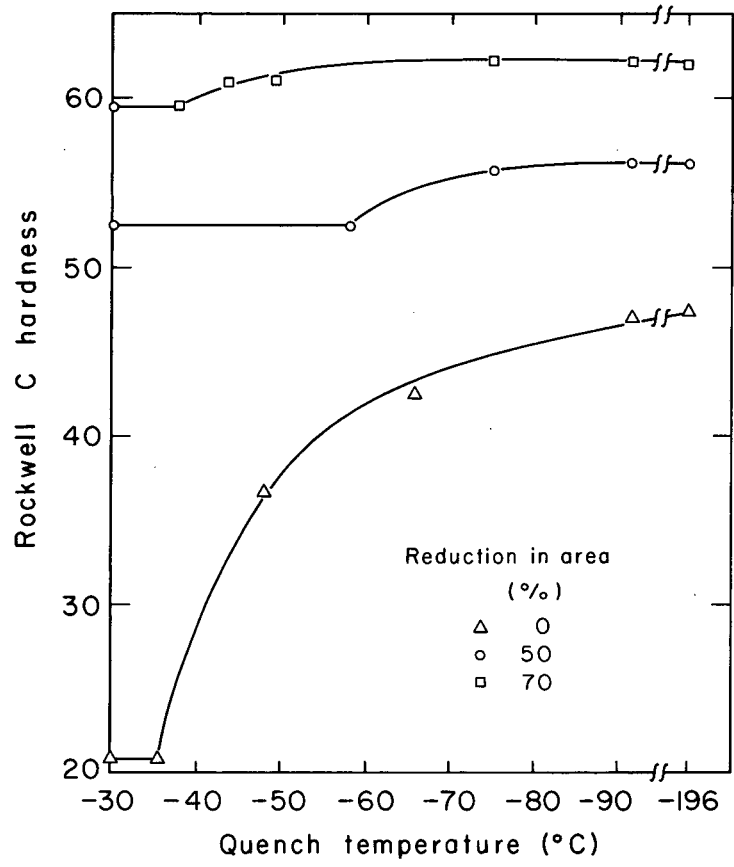
MUB-7282
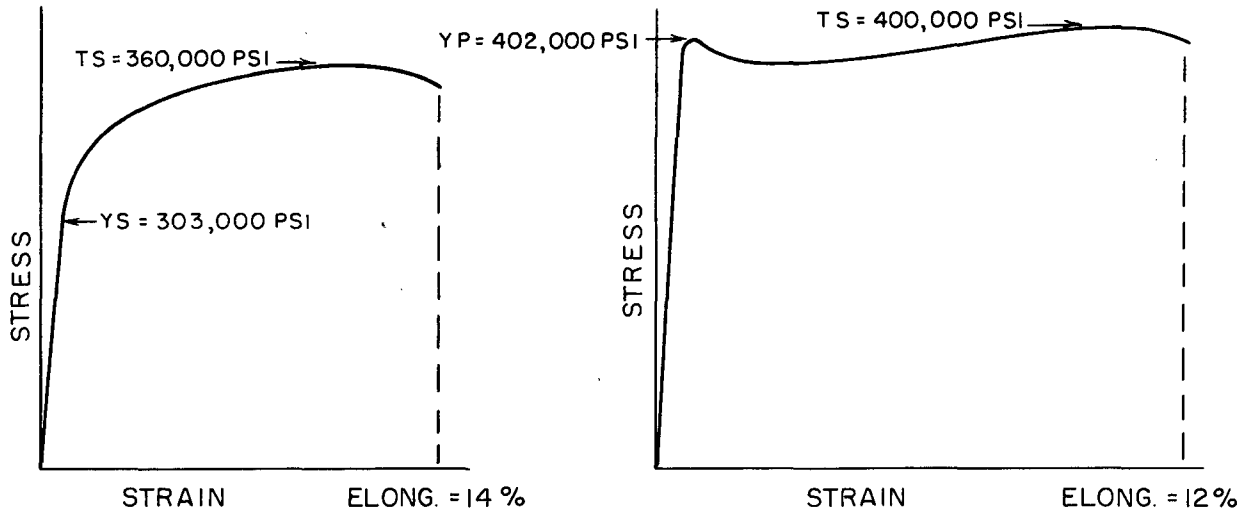
81 Pt − 19 Au
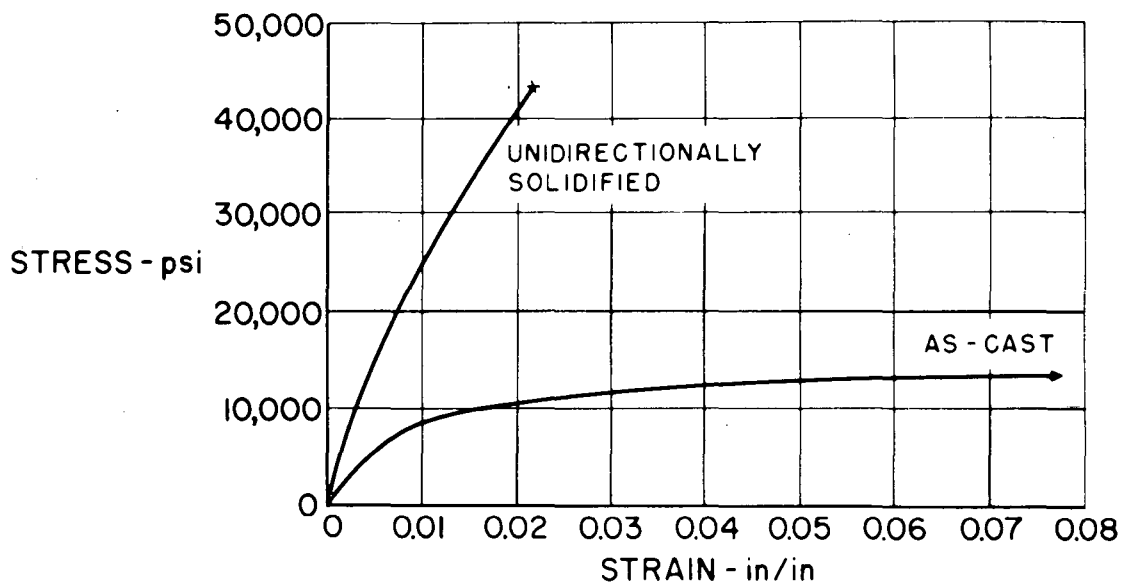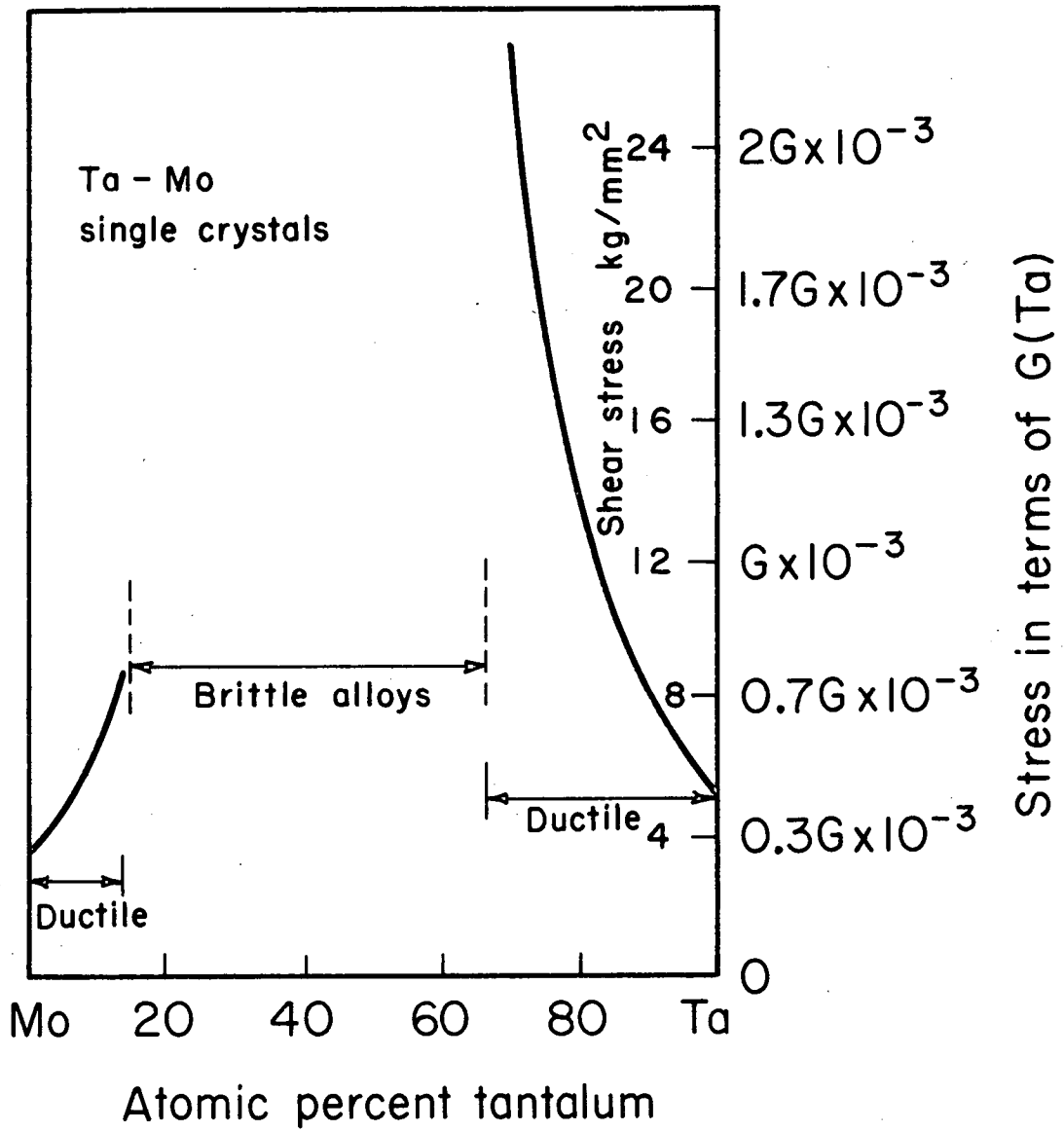
MUB-7272

Fig. 17

ZN-4630

Fig. 18 a

ZN-5175

Fig. 18b

Fig. 19

MUB-7271
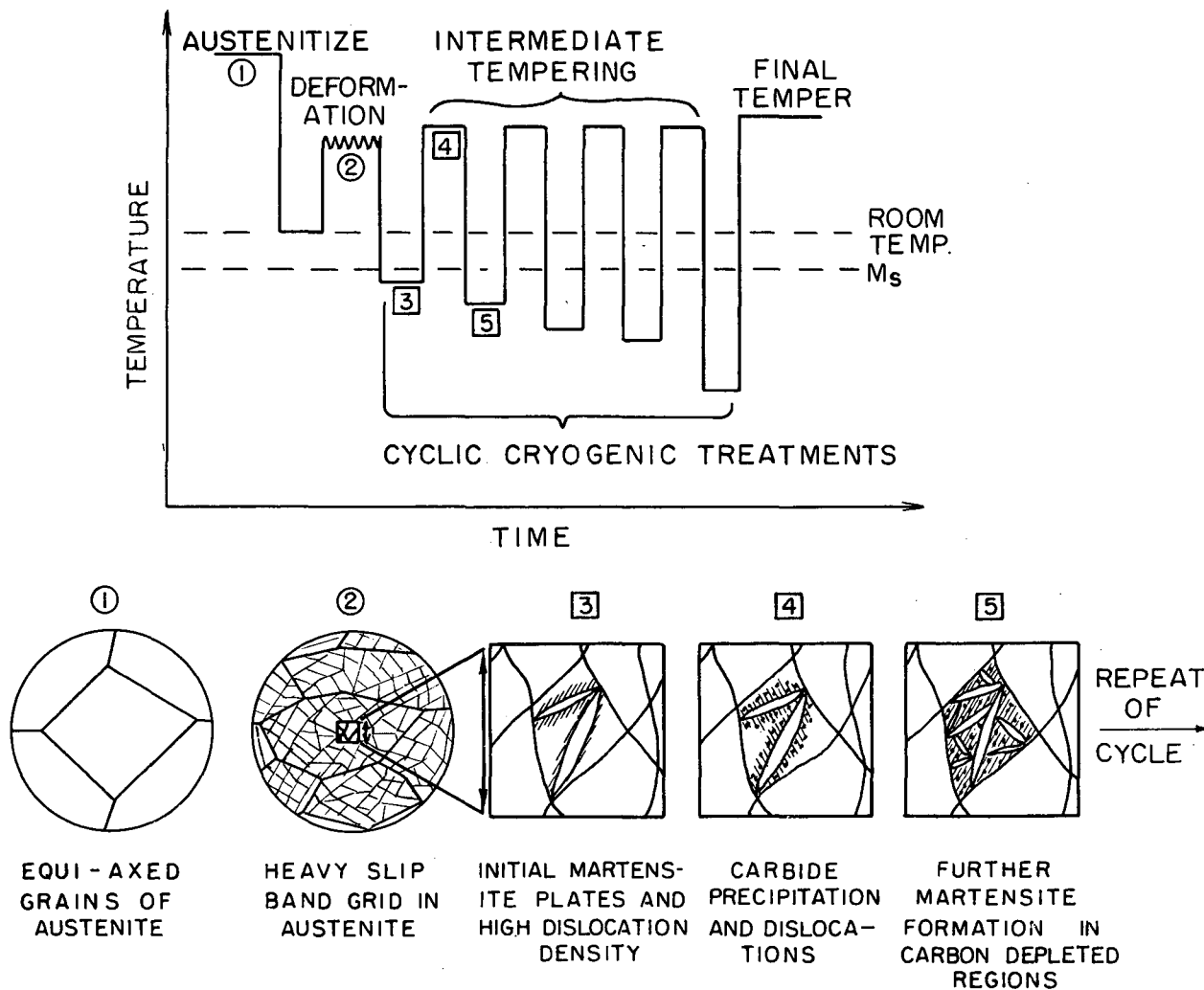
Fig. 20a

Fig. 20 b

AUSFORMED H-11 STEEL
DEFORMED 80%, QUENCHED
AND TEMPERED AT 600°F
TESTED AT 70°F.

AUSFORMED H-11 STEEL DEFORMED
80%, QUENCHED AND TEMPERED AT
600°F, STRAINED 2% AT 300°F,
AGED AT 600°F, TESTED AT 70°F.

MUB-3065

Fig. 21